Key Points:
- We analyze intraplate deformation driven by mantle lithosphere heterogeneities and compare to crustal inheritance deformation
- We find that during compression the strength of the mantle lithosphere is integral in generating deformation from a structural anomaly
- If the mantle lithosphere is strong with ubiquitous weak zones, it is a viable candidate to be the fundamental control on the Wilson Cycle

Correspondence to:
P. J. Heron,
philip.heron@utoronto.ca

Identifying mantle lithosphere inheritance in controlling intraplate orogenesis

Philip J. Heron[1], Russell N. Pysklywec[1], and Randell Stephenson[2]

[1]Department of Earth Sciences, University of Toronto, Toronto, Ontario, Canada, [2]School of Geosciences, University of Aberdeen, Aberdeen, Scotland

Abstract Crustal inheritance is often considered important in the tectonic evolution of the Wilson Cycle. However, the role of the mantle lithosphere is usually overlooked due to its difficulty to image and uncertainty in rheological makeup. Recently, increased resolution in lithosphere imaging has shown potential scarring in continental mantle lithosphere to be ubiquitous. In our study, we analyze intraplate deformation driven by mantle lithosphere heterogeneities from ancient Wilson Cycle processes and compare this to crustal inheritance deformation. We present 2-D numerical experiments of continental convergence to generate intraplate deformation, exploring the limits of continental rheology to understand the dominant lithosphere layer across a broad range of geological settings. By implementing a "jelly sandwich" rheology, common in stable continental lithosphere, we find that during compression the strength of the mantle lithosphere is integral in generating deformation from a structural anomaly. We posit that if the continental mantle is the strongest layer within the lithosphere, then such inheritance may have important implications for the Wilson Cycle. Furthermore, our models show that deformation driven by mantle lithosphere scarring can produce tectonic patterns related to intraplate orogenesis originating from crustal sources, highlighting the need for a more formal discussion of the role of the mantle lithosphere in plate tectonics.

1. Introduction

In 1966, based on evidence in the fossil record and the dating of vestiges of ancient volcanoes, *Wilson* [1966] proposed a cycle describing the opening and closing of oceanic basins and therefore a method of amalgamating continental material (into a supercontinent) that would be subsequently dispersed (e.g., into the present-day continental configuration). *Wilson* [1966], building on previous studies [e.g., *Hess*, 1962; *Vine and Matthews*, 1963; *Wilson*, 1965], outlined a four-stage "Wilson Cycle" (as it was later named by *Dewey and Burke* [1974]): the dispersal (or rifting) of a continent; continental drift, seafloor spreading, and the formation of oceanic basins; new subduction initiation and the subsequent closure of oceanic basins through oceanic lithosphere subduction; and continent-continent collision and closure of the oceanic basin (Figure 1). The Wilson Cycle was later extrapolated to the larger-scale processes involved in the supercontinent cycle [e.g., *Nance and Murphy*, 2013].

Over the past 50 years this conventional theory of plate tectonics has been at the forefront of geodynamics. However, many features of lithosphere evolution fall outside the realm of the Wilson Cycle: plate tectonics has progressed beyond plate boundaries as the sole locus of major deformation with the study of intraplate orogenesis [e.g., *Sykes*, 1972, 1978; *Smith and Bruhn*, 1984; *Sibson*, 1992; *Ziegler et al.*, 1995, 1998; *Stein and Liu*, 2009; *Stephenson et al.*, 2009]; mantle lithosphere processes generating lithospheric instabilities (in the form of viscous dripping and delamination) that represent a foundering and recycling of plate material [e.g., *Bird*, 1979; *Houseman et al.*, 1981, 1997; *Göğüş and Pysklywec*, 2008; *Bajolet et al.*, 2012; *Göğüş et al.*, 2016] and in situ mantle lithosphere inversion of Archean cratonic keels [*Percival and Pysklywec*, 2007]; and the interaction of subduction and large low shear velocity provinces in driving the development of large igneous provinces at the surface [e.g., *Ernst et al.*, 2005; *McNamara and Zhong*, 2005; *Bull et al.*, 2009; *Heron et al.*, 2015a; *Mallard et al.*, 2016].

Among these, the study of intraplate orogenesis has generated a number of mechanisms for deformation within a plate interior (Figure 1). These mechanisms include preexisting lithosphere structures, the presence of fluids, the burial of highly radiogenic material and other temperature anomalies, mantle lithosphere
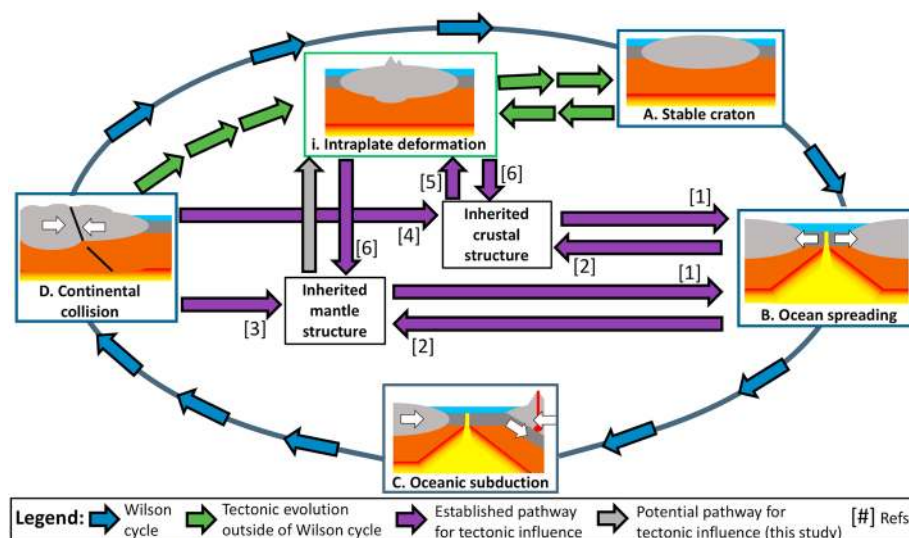
Figure 1. The Wilson Cycle with an additional tectonic feature of intraplate deformation. Rifting (B), continental collision (D), and/or intraplate deformation (i) can leave lasting impressions on the crust and mantle. The importance of inherited crustal and mantle structures in influencing the tectonic pathway of deformation is shown by purple arrows. The grey arrow shows the focus of this study, analyzing the potential influence of existing mantle structures (from B, D, or i) on intraplate deformation, and whether they can be distinguished from inherited crustal structure. The references for the established pathway tectonic influence are as follows: [1] *Huismans and Beaumont* [2011]; [2] *Royden and Keen* [1980], *Davis and Kusznir* [2004], *Buiter et al.* [2009], and *Péron-Pinvidic et al.* [2013]; [3] *Flack and Warner* [1990], *Morgan et al.* [1994], *Lie and Husebye* [1994], *Calvert et al.* [1995], *Calvert and Ludden* [1999], *Ghazian and Buiter* [2013], and *Schiffer et al.* [2014, 2016]; [4] *Tapponnier and Molnar* [1975]; [5] *Stephenson et al.* [2009] and *Buiter et al.* [2009]; and [6] *Cowgill et al.* [2003], *Dèzes et al.* [2004], *Avouac et al.* [1993], *Cowgill et al.* [2003], *Tapponnier and Molnar* [1975], and *Kahraman et al.* [2015]. The role of plumes in the Wilson Cycle is not discussed in this figure or manuscript.

instability, compositional strengthening, and strain rate [e.g., *Ziegler*, 1987; *Ziegler et al.*, 1995, 1998; *Sandiford*, 1999; *Nielsen and Hansen*, 2000; *Hansen and Nielsen*, 2002; *Pysklywec and Beaumont*, 2004; *Sandiford et al.*, 2006; *Stephenson et al.*, 2009; *Heron and Pysklywec*, 2016]. In this study, we examine the role of deep, long-lived inherited lithospheric structures in deformation away from plate boundaries to allow for a greater understanding of the modern view of the conventional theory of plate tectonics (e.g., Figure 1).

It is widely believed that inherited crustal structures influence tectonic evolution of the Wilson Cycle [e.g., *Wilson*, 1966; *Thomas*, 2006; *Stephenson et al.*, 2009; *Buiter et al.*, 2009; *Huismans and Beaumont*, 2011], as described in Figure 1. The source of intraplate orogenesis is also discussed in terms of preexisting crustal structures influencing deformation, generating crustal thickening beyond plate boundaries [e.g., *Murphy et al.*, 1997; *Roberts and Houseman*, 2001; *Collins*, 2002; *Pysklywec and Beaumont*, 2004; *Jammes and Huismans*, 2012; *Wang et al.*, 2013]. However, through seismic imaging and geochemical analysis, the mantle lithosphere is also known to be disturbed or "scarred" [e.g., *Wendlandt et al.*, 1993; *Lee et al.*, 2001; *Yuan and Romanowicz*, 2010; *Lee et al.*, 2011; *Hopper and Fischer*, 2015] with deep inherited structures often interpreted to be the result of closure of ocean basins and continental collisions [e.g., *Flack and Warner*, 1990; *Klemperer and Hobbs*, 1991; *Lie and Husebye*, 1994; *Morgan et al.*, 1994; *Guellec et al.*, 1990; *Pfiffner*, 1992; *Calvert et al.*, 1995; *Calvert and Ludden*, 1999; *Cook et al.*, 1999; *van der Velden and Cook*, 2002; *Cook*, 2002; *Cook and Vasudevan*, 2003; *White et al.*, 2003; *Cook et al.*, 2004; *van der Velden and Cook*, 2005; *Schiffer et al.*, 2014, 2015, 2016]. The ages of these mantle lithosphere damage structures vary, with some features thought to be of Archean age [e.g., *Calvert et al.*, 1995]. The majority of the deep heterogeneities can be found continental interiors [e.g., *Steer et al.*, 1998; *Heron et al.*, 2016].

Although tectonic processes have shown to impact on the mantle lithosphere [e.g., *Wendlandt et al.*, 1993; *Lee et al.*, 2001; *Yuan and Romanowicz*, 2010; *Lee et al.*, 2011; *Hopper and Fischer*, 2015], deep inheritance as a source of intraplate deformation (and as a process within the Wilson Cycle as a whole) is often overlooked. One reason for this is the ambiguity in the rheological properties of the scars after being "frozen" into the lithosphere.

Schiffer et al. [2016] discuss mantle lithosphere scarring on the continental margin of East Greenland as being denser in composition as compared to the surrounding mantle material. However, a number of studies have discussed the weakening impact of tectonic processes on the lithosphere to facilitate continental rifting [*Dunbar and Sawyer*, 1988, 1989]. Furthermore, the subduction of crustal material into the mantle through ancient processes could increase volatiles to the lower lithosphere, weakening the seismically imagined scarred material [*Pollack*, 1986]. The propensity of continents to break apart parallel to ancient orogenic belts also indicates a role of inherited structures in controlling tectonics, with rheological heterogeneity and mechanical anisotropy playing a role [*Vauchez et al.*, 1997, 1998]. As a result, it is appropriate to interpret the seismic imaging of scarring to be regions of weakness in the continental mantle [e.g., *Linckens et al.*, 2015; *Heron et al.*, 2016].

The role of grain damage in tectonic processes is also a method by which weakening could occur in the mantle lithosphere. Deformation related to subduction has been inferred to generate a reduction in grain size through the continuum theory of damage mechanics [*Bercovici and Ricard*, 2014; *Krajcinovic*, 1996]. For this study, we interpret the seismic imaging of mantle lithosphere heterogeneities to be ancient deformation, with the reduction in grain size acting as a weak plane [*Bercovici and Ricard*, 2014]. There is geochemical precedence for this, with mantle lithosphere peridotite mylonites showing a reduction in grain size at plate boundaries — related to tectonic deformation [*Skemer et al.*, 2010; *Warren and Hirth*, 2006; *Linckens et al.*, 2015]. Deep earthquakes have also been linked to reduced grained low-viscosity planes from ancient subduction processes, leading to slip over time [e.g., *Ogawa*, 1987; *Wiens*, 2001; *Kelemen and Hirth*, 2007; *Prieto et al.*, 2013]. Furthermore, lithospheric damage related to inheritance has been inferred to remain weak over very long timescales [*Audet and Bürgmann*, 2011], allowing ancient processes related to Archean scarring to be considered in present-day tectonics.

Implementing self-consistent grain damage as a driver for plate tectonic processes is beyond the scope of this study, as the timescale for reactivation of scarring may occur over hundreds of millions of years. In this study, we model preexisting zones of weakness (i.e., lithospheric scars) by specifying a region with a low angle of internal friction to mirror the processes of lithospheric damage and simulate inherited structures in the upper crust (UC), lower crust (LC), and mantle lithosphere (ML).

Intraplate orogenesis has often been described in terms of processes that eventually lead to crustal thickening [*Murphy et al.*, 1997; *Roberts and Houseman*, 2001; *Collins*, 2002; *Pysklywec and Beaumont*, 2004; *Jammes and Huismans*, 2012; *Wang et al.*, 2013]. Here we posit that if a number of processes originating in the crust and/or mantle lithosphere can lead to crustal thickening, how can the source of intraplate orogenesis be resolved (e.g., Figure 1)? The analysis of structures in the mantle lithosphere has increased in recent years, with the advent of better imaging techniques [*Schaeffer and Lebedev*, 2015]. As a result, more structures within the mantle lithosphere have become visible [*Zhang et al.*, 2014; *Hopper and Fischer*, 2015; *Kahraman et al.*, 2015; *Gilligan et al.*, 2016; *Schiffer et al.*, 2016], permitting a more focused look at subcrustal architecture impacting surface tectonics. Furthermore, a number of recent studies have indicated the mantle lithosphere (and deeper) to be important in plate tectonics [*Bercovici and Ricard*, 2014; *Leng and Gurnis*, 2015; *Becker et al.*, 2015; *Chamberlain et al.*, 2014; *VanderBeek et al.*, 2016; *Gilligan et al.*, 2016]. Despite this, many studies have failed to acknowledge the role of the mantle lithosphere in plate tectonic processes and in particular its role within the Wilson Cycle. The work presented here highlights the need for a more formal look at subcrustal tectonics in the context of the conventional theory of plate tectonics (Figure 1).

2. Method

2.1. Governing Equations

The experiments are modeled using the two-dimensional, thermal-mechanical finite element numerical code SOPALE [*Fullsack*, 1995], which implements an Arbitrary Lagrangian-Eulerian (ALE) method to solve for the deformation of high Prandtl number incompressible viscous-plastic media (the model does not include elastic deformation). The governing hydrodynamic equations for the numerical models include the equations of conservation of mass, momentum, and internal energy, respectively

$$\nabla \cdot \mathbf{u} = 0, \tag{1}$$

$$\nabla \cdot \underline{\underline{\sigma}} + \rho g = 0, \tag{2}$$

$$\rho c_p \left(\frac{\partial T}{\partial t} + \mathbf{u} \cdot \nabla T \right) = k \nabla^2 T + H. \tag{3}$$

In the equations above **u** (m s^{-1}), $\underline{\underline{\sigma}}$ (Pa), ρ (kg m^{-3}), g (m s^{-2}), c_p (J kg^{-1} K^{-1}), T (K), k (W m^{-1} K^{-1}), H (W m^{-3}), and t (s) are the velocity, stress tensor, density, gravitational acceleration, specific heat capacity, temperature, thermal conductivity, volumetric rate of internal heat production, and time, respectively. The system is completed by an associated linearized equation of state:

$$\rho = \rho_o(1 - \alpha(T - T_o)), \tag{4}$$

where α is the coefficient of thermal expansion, ρ_o is the reference material density, and T_o is the reference temperature.

The stress tensor in equation (2) may be divided into the deviatoric stress tensor, σ', and a pressure term,

$$\sigma_{ij} = \sigma'_{ij} - \delta_{ij}P, \tag{5}$$

where for an incompressible fluid, δ is the Kronecker delta and P is the pressure (which is given as $-\frac{1}{3}\sigma_{ii}$). The deviatoric stress is determined at each computational node (in parallel) as the lesser value of a yield stress, σ_y, or viscous stress, σ_v. In the numerical code, the frictional plastic yield stress is given by a pressure-dependent incompressible Drucker-Prager yield criterion

$$\sigma_y = P\sin(\phi) + C_o, \tag{6}$$

where ϕ is the angle of internal friction and C_o the cohesion. The viscous stress is given by

$$\sigma_v = 2\eta_e \dot{I}'_2, \tag{7}$$

where $\dot{I}'_2$ is the second invariant of the deviatoric strain rate tensor and η_e the effective viscosity. When the thermally activated power law creep is used, the effective viscosity is given as

$$\eta_e = \left(3^{\frac{-(1+n)}{2n}} 2^{\frac{1-n}{n}}\right) fA^{\frac{-1}{n}} \left(\dot{I}'_2\right)^{\frac{(1+n)}{2n}} e^{\frac{Q}{nRT}} \tag{8}$$

where A is the material constant, f is a scaling parameter, n is the power law exponent, Q is the thermal activation energy, R is gas constant, and T is the temperature.

The ALE method applies a Lagrangian grid (resolution 801 × 649) and a Eulerian grid (resolution 401 × 217) and allows moving material interfaces (such as a free surface and internal chemical boundaries) in a high-strain environment. The models are set up by defining disparate material regions (e.g., upper crust, lower crust, mantle lithosphere, and asthenosphere) on a Lagrangian mesh. This information is mapped onto the Eulerian grid where the governing equations are solved for the flow velocity, pressure, and temperature. After subsequently mapping this information back onto the Lagrangian grid, the interpolated velocity on the higher-resolution mesh is used to advect the thermal and material properties, whereupon the coupled Lagrangian-Eulerian interaction is repeated [e.g., *Fullsack*, 1995]. The Eulerian domain is restricted to small vertical dilations (corresponding to the evolution of topography on the free upper surface) and therefore is used as a "solver grid," while the advecting Lagrangian grid is used to track deforming material.

The accuracy of SOPALE has been verified by an extensive series of benchmarking models from previous numerical experiments [e.g., *Fullsack*, 1995]. The computational code has been shown to be in agreement with other numerical and analytical studies [*Houseman and Molnar*, 1997; *van Keken et al.*, 1997; *Buiter et al.*, 2006, 2016].

2.2. The Initial Model Setup

Figure 2 shows the setup of the reference case for modeling intraplate deformation. We model the upper and lower crust, the mantle lithosphere, and portion of the sublithospheric mantle in 1500 km width and 600 km depth two-dimensional numerical experiments. In the standard model, the LC, UC, and ML have thicknesses of 24 km, 12 km, and 114 km, respectively.

The models consider convergence in a stable (i.e., strong) [*Burov and Watts*, 2006] continental crust and mantle lithosphere setting where the majority of mantle lithosphere scars are found [e.g., *Steer et al.*, 1998; *Heron et al.*, 2016] (material properties given in Table 1). The model setup allows for a heterogeneous lithosphere, with a number of different weak zones (Figure 2b).

An initial (laterally uniform) temperature field (i.e., a geotherm) is prescribed for all models. The geotherm has the surface and basal temperature fixed throughout the duration of the model runs (at 20°C and 1570°C for
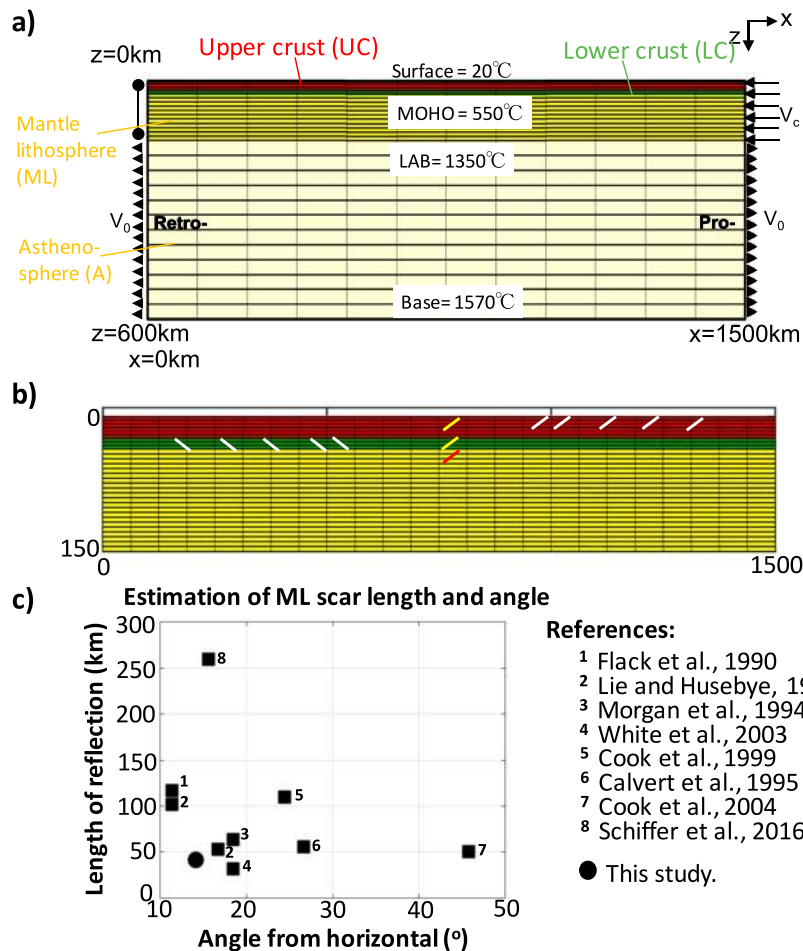
Figure 2. The initial setup of the models. (a) Upper crust (denoted by red has a thickness of 24 km), lower crust (green, thickness 12 km), mantle lithosphere (yellow, thickness 114 km), and sublithospheric mantle (beige, the bottom 450 km) have corresponding physical parameters as given in Table 1. Initially, the temperature of the model increases linearly throughout the solution domain (as shown in Figure 2a). The Lagrangian and Eulerian grid resolutions are 801×649 and 401×217, respectively. The Lagrangian grid (black mesh) is only partially represented here and shows that 17% and 39% of the grid occupy the crust and mantle lithosphere, respectively (the same ratios apply to the Eulerian grid). Continental convergence is incorporated by introducing new lithosphere at the right boundary of box with velocity $v_c = 1$ cm yr^{-1}. (b) Positions of scars used in this study. In the majority of cases, weak zones (scars) in the UC and LC (as shown in white) and ML (red). Yellow crustal scars are used in Figures 6 and 10. All weak zones are specified as having a 1° angle of internal friction (unless stated). (c) Estimation of mantle lithosphere scar length and angle from horizontal for eight examples of ML heterogeneities.

the standard model, respectively). However, as both the mechanical and thermal calculations are carried out for each time step, the interior temperature field can evolve over space and time and is not fixed to the preliminary geotherm. Initially (for the standard model), a linear temperature increase of 20°C to 550°C from the surface to the Moho depth is imposed, with a further linear temperature increase to 1350°C at the base of the lithosphere. Radiogenic heat production occurs within the crust, with the majority of internal heat generation coming from the upper crust (2.1 μW m^{-3}) [e.g., *Beaumont et al.*, 2004] rather than the lower crust (0.7 μW m^{-3}). The effect of the initial temperature setup on crustal deformation is explored in suites of numerical models in section 3.2.

Creep in the model is driven by internal buoyancy forces and an imposed plate motion. In the standard model, plate motion is modeled by introduced new lithosphere into the domain at a horizontal velocity of $v_c = 1$ cm yr^{-1} (Figure 2). The left margin of all models is held fixed, while a small outward flux, v_o, maintains the mass balance of the system (Figure 2). Neither surface erosion nor deposition is considered in this study.

Table 1. Rheological Parameters Used for the Continental Collisions in the Manuscript[a]

	C_o	ϕ_2	ϕ_1	$\left(I_2'\right)^{\frac{1}{2}}_1$	$\left(I_2'\right)^{\frac{1}{2}}_2$	A	f	Q	n	Ref	ρ_o	T_0
UC	10^6	15°	2°	0.5	1.5	1.4×10^{-28}	0.3	223	4	1	2700	293
LC	10^6	15°	2°	0.5	1.5	4.4×10^{-29}	0.05	485	4.7	2	2900	293
ML	10	15°	2°	0.5	1.5	8.3×10^{-18}	0.3	535	3.5	3	3250	1609
SM	10	15°	2°	0.5	1.5	8.3×10^{-18}	0.3	535	3.5	3	3250	1609
WZ		1	0.5									

[a]Upper crust, lower crust, mantle lithosphere, the sublithospheric mantle, and a weak zone are denoted by UC, LC, ML, SM, and WZ, respectively. Symbols are as parameters given in the text (units for C_o, A, Q, ρ_o, and T_0 are Pa, Pa^{-n} s^{-1}, kJ mol^{-1}, K kg m^{-3}, and K). $\left(I_2'\right)^{\frac{1}{2}}$ is accumulated strain. Reference list for Ref are as follows: (1) *Gleason and Tullis* [1995], (2) *Ranalli* [1997], *Mackwell et al.* [1998], (3) *Hirth and Kohlstedt* [1996], and *Kawazoe et al.* [2009]. The flow laws that represent each region are wet quartzite for UC, Maryland diabase for LC, and dry olivine for ML and SM. For WZ the flow law is governed by the host material (with a prescribed $\phi_e = 1°$). Physical parameters that remain constant across all regions are $\alpha = 3 \times 10^{-5}$ K^{-1}, $k = 2.25$ W m^{-1} K^{-1}, and $c_p = 750$ J k g^{-1} K^{-1}. The upper crust and lower crust have radioactive heat production values of 2.1 µW m^{-3} and 0.7 µW m^{-3}, respectively. The viscosity range for the model is $1 \times 10^{20} - 1 \times 10^{27}$.

2.3. Rheological Parameters

We test the limits of mantle lithosphere dominating intraplate tectonics by changing the rheological parameters of the ML and LC to generate a range of strengths within the lithosphere. The effective viscosity equation (for viscous flow, equation (8)) has a scaling factor (f) that is used to change the strength of the material (e.g., to simulate "wet" (a low f value) and "dry" materials (high f)). The standard values for the scaling factor were chosen to be consistent with previous numerical experiments of continental collisions in strong mantle lithosphere rheologies [*Beaumont et al.*, 2004; *Burov and Watts*, 2006; *Göğüş and Pysklywec*, 2008; *Huismans and Beaumont*, 2011; *Burov*, 2011; *Gray and Pysklywec*, 2012; *Wang et al.*, 2014; *Heron et al.*, 2015b, 2016]. As there are uncertainties in the derived material parameters, we also use the scaling factor to cover all types of lithospheric strength profiles. For the ML, we modify f from 1.0 (the standard value) to as high as 100 and as low as 0.01. For LC, a low scaling factor of 0.05 is used for the standard value to obtain a "jelly sandwich" continental rheology. The UC scaling is set at 0.3 throughout the study.
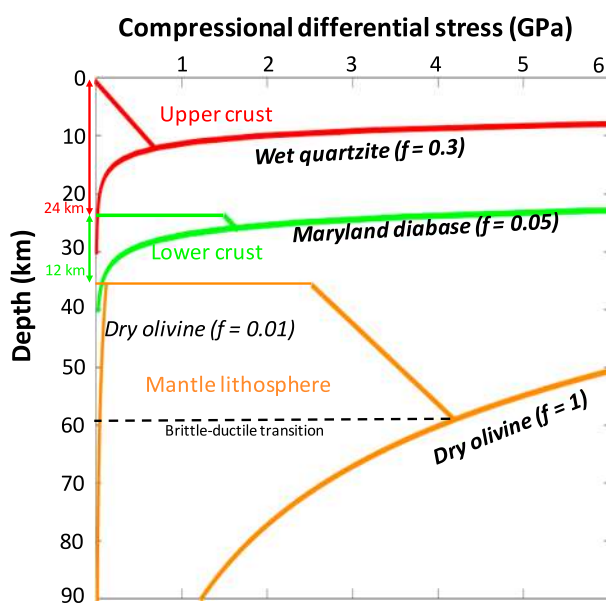

Figure 3. Yield stress envelopes for the different rheological layers. Brittle yield stress and ductile yield stress are calculated as in text, using parameters from Table 1 and an initial geotherm of 15°C km^{-1} from the surface to 36 km and 7°C km^{-1} from the 36 km to 90 km. The bold markers refer to the standard model used in the manuscript.
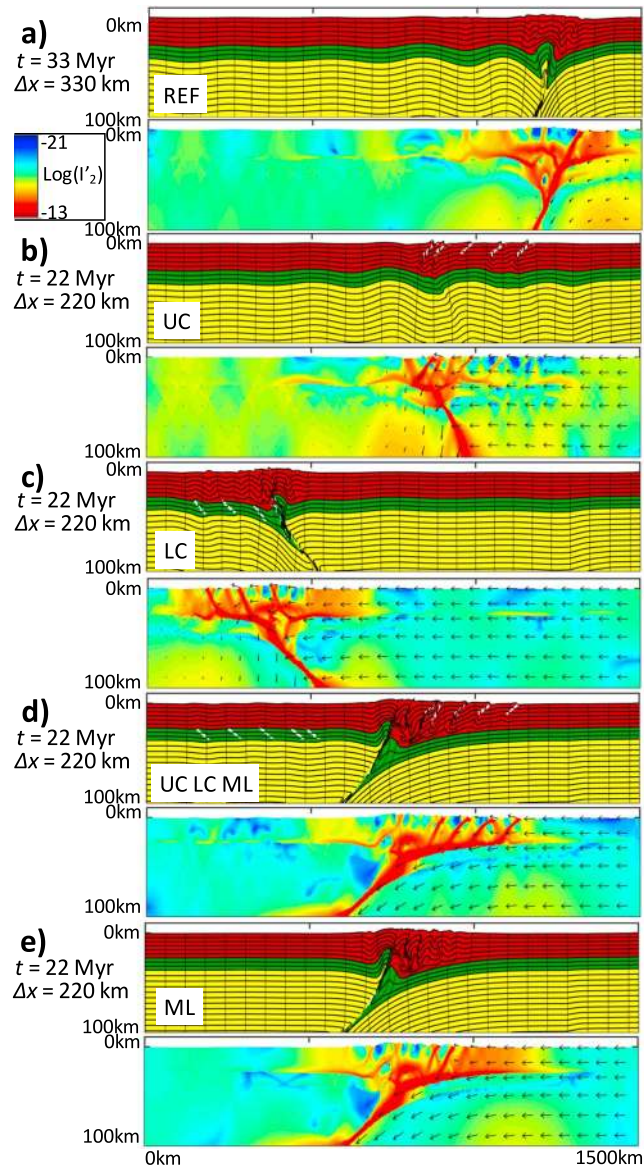
Figure 4. Compression model results for combinations of weak scars using the standard rheological set up (Table 1). Material deformation (top) and visualization of the second invariant of the deviatoric strain rate tensor (bottom) after shortening for (a) a model without any scarring, (b) model with UC scar only, (c) model with LC scar only, (d) model with all scars (e.g., Figure 2b), and (e) model with a ML scar only. Top 100 km of the models are shown in a 3X vertical exaggeration.

Figure 3 shows the range of lithospheric strength versus depth for the standard model used in this study. The brittle strength for a compressional regime is given by

$$\sigma_{\mathrm{brittle}}(z) = 2\left[C_o \frac{\cos \phi}{1 - \sin \phi} + \rho z (1 - \lambda)\left(\frac{\sin \phi}{1 - \sin \phi}\right)\right], \qquad (9)$$

where $\sigma_{\mathrm{brittle}}$ is the brittle deviatoric yielding stress, C_o is the cohesion, ϕ is the angle of internal friction, ρ is the average density of the layer, and λ is the pore fluid ratio. Here we follow *Mouthereau et al.* [2006] in applying a hydrostatic condition for pore fluid ratio ($\lambda = 0.4$). In all layers the ϕ is given as 15°, with strain softening to 2° (Table 1). Thermally activated dislocation creep [*Brace and Kohlstedt*, 1980] is given by

$$\sigma_{\mathrm{ductile}} = f\left(\frac{\dot{\varepsilon}}{A}\right)^{1/n} \exp\left(\frac{Q}{nRT}\right), \qquad (10)$$

where f, n, A, and Q are the scaling factor, power law exponent, material constant, and thermal activation energy, respectively (as given in Table 1). A geotherm of 15°C km^{-1} in the crust and 7°C km^{-1} in the mantle is used to calculate the ductile lithospheric strength alongside a representative strain rate of 10^{-15} s^{-1}.

2.4. The Weakness and Geometry of Lithosphere Scars

All weak zones have the same material properties as the layer they occupy (Table 1), but with a very low value for the internal angle of friction ($\phi = 1°$) (unless specified). By this method, all faults are equally primed to fail due to the low brittle strength.

Our choice of mantle lithosphere and crustal scar geometry is conservative, compared to the seismic imaging indication of the mantle lithosphere scars, to preserve the equality of the scarring among the layers. As a result, there is a trade-off between having large crustal features and smaller mantle lithosphere heterogeneities. We choose a more representative value for this study and also test the extremes to show to what extent the study is based on scar geometry (e.g., Figure 11).

The same geometry is used for all the UC, LC, and ML weak zones in the standard model, with scars angled 14° below the horizontal for 41 km (10 km deep, 40 km in length, and 10 km width). Figure 2c shows an approximation of the length and angle from horizontal for eight examples of ML scars. The values were obtained by measuring the horizontal and vertical extent of the mantle reflections from the cross sections in the studies. As a result, they are first-order estimations. A recent high-density seismometer array study showed horizontal structural variations in the crust and upper mantle to be less than 10 km and 20 km, respectively [*Kahraman et al.*, 2015]. Our models take such width dimensions of heterogeneity into consideration when implementing lithosphere scarring.

The seismic reflections measured from Figure 2c can be categorized into continental interior scars (points 1 to 6) and continental margin scars (7 and 8). The continental interior heterogeneities are less than 130 km in length and have an angle lower than 30° from the horizontal. The two continental margin reflectors show a more varied scar geometry, with a high length and low angle [*Schiffer et al.*, 2016] or short length and high angle [*Cook et al.*, 2004], and represent outliers for this study (Figure 4c).

2.5. Model Summary

Our results present suites of models to highlight how the dominance of mantle lithosphere scarring on tectonics can be identified over crustal inheritance. In section 3.1, we study the style of tectonics generated from mantle lithosphere scarring reactivating in response to shortening, in comparison to deformation generated from crustal heterogeneities. Section 3.2 explores the limits at which a mantle lithosphere scar would be dominant in intraplate orogenesis. The role of the "jelly" in the jelly sandwich rheology is analyzed in section 3.3 to understand how a weak lower crust could impact deformation in the surrounding layers. The strength of the mantle lithosphere and the geometry of deep scarring are explored in section 3.4.

3. Results

3.1. Mantle Lithosphere Dominance: Style, Timing, and Depth

Figure 4 shows examples of deformation related to the different scarring within the lithosphere (UC, LC, UC LC ML, and ML), as well as a reference case where a homogeneous lithosphere is shortened ("REF"). In a continental compression model featuring no crust or mantle lithosphere heterogeneities (REF, Figure 4a), the crust and mantle lithosphere shortens through the development of a series of shear zones due to the build up of stress. Crustal faulting propagates away from the initial deformation region as shortening continues, with high strain rate occurring across the crust and mantle lithosphere (Figure 4a).

In Figures 4b–4e, crustal and mantle lithosphere inheritance is prescribed from Figure 2b as shown by the white scars and red heterogeneity, respectively. This configuration of the upper crust and lower crust weak zones permits easy identification of which layer is controlling deformation. After considerable shortening (in keeping with the extent of similar tectonic scenarios) [e.g., *Cowgill et al.*, 2003], crustal thickening and faulting, key characteristics of intraplate orogenesis, are shown in models that feature UC or LC scars (Figures 4b and 4c). The implementation of a weak scar in the mantle lithosphere (overlain by a heterogeneous crust) dominates tectonics for this jelly sandwich rheology (Figure 4d). The impact of crustal scars is minimal when in the presence of a mantle lithosphere scar, as shown by comparing Figure 4d, featuring UC, LC, and ML scars, with Figure 4e, one ML scar only.
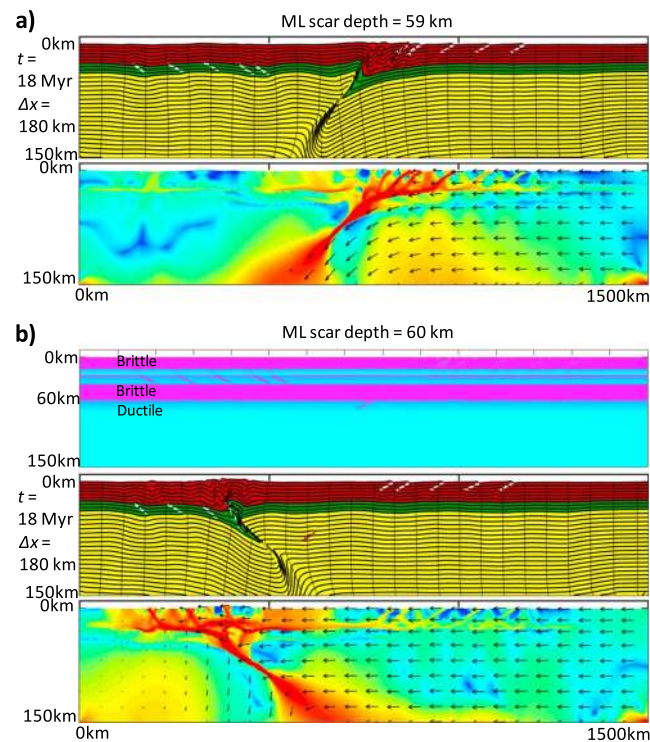
Figure 5. Difference in applying the mantle lithosphere weak zone at (a) 59 km and (b) 60 km depth with upper and lower crust scars. Material and strain rate plots are shown, as well as in (b) the norm of deviatoric stress tensor divided by the plastic yield level to show brittle flow (pink) and ductile flow (blue). At 59 km, the deformation is related to the mantle lithosphere scar, while at 60 km (e.g., Figure 4c), the model deforms in a lower crust style (e.g., Figure 4d).

The impact of the mantle lithosphere scar is linked to the strength of the layer and the rheological flow regime. In the standard model, we implement a jelly sandwich rheology, as shown in Figure 3. The scars in all layers of the lithosphere exist within a brittle flow regime, the reactivation of which localizes stresses. The brittleness of the lithosphere, rather than the ductile flow, facilitates deformation.

Figure 5 tests the limits to which mantle lithosphere structures could have influence, using the britlte-ductile flow transition as a guide (Figure 3). Figure 5a presents continental convergence featuring UC, LC, and ML scars (as Figure 4d), but with the mantle lithosphere heterogeneity located at the boundary of brittle-ductile flow (59 km). The brittle nature of the strong mantle lithosphere controls deformation (Figure 5a). Positioning the mantle lithosphere scar fully within the ductile layer of the lithosphere, at 60 km as shown in Figure 5b, neutralizes the influence of the heterogeneity. The strong lower crust (Figure 3) dominates over the upper crust scarring, as brittle layering within the lower crust reactivates the heterogeneities. Strength of the layers can be seen as important in determining the tectonic influence on deformation.

Having understood the dominance of rheological brittle strength of the lithosphere to generate deformation in Figures 4 and 5, Figure 6 explores the timing and deformation pattern using the yellow crustal scars and mantle lithosphere scar shown in Figure 2b. By positioning the various lithosphere scars in the same horizontal location, the differences in tectonic styles can be identified.

After 300 km of shortening, UC (Figure 6a), LC (Figure 6b), and UC, LC, and ML models (Figure 6c) all produce similar tectonic patterns. Thickening of the upper and lower crust impacts on the mantle lithosphere below to produce a deep shear. Although some folding and faulting may differ in the upper crust, all models produce a typical intraplate orogenesis pattern of thickened crust. After sufficient shortening, this thickened crust impacts on the mantle lithosphere generating deformation. The strength of the mantle lithosphere plays a role in this tectonic progression, with brittle deformation occurring even without the presence of a deep scar (Figures 6a and 6b).

The timing of the onset of mantle lithosphere shear differs between the models. A UC scar takes the most amount of shortening (300 km) to eventually impact on the mantle lithosphere below (Figure 6a), with a LC
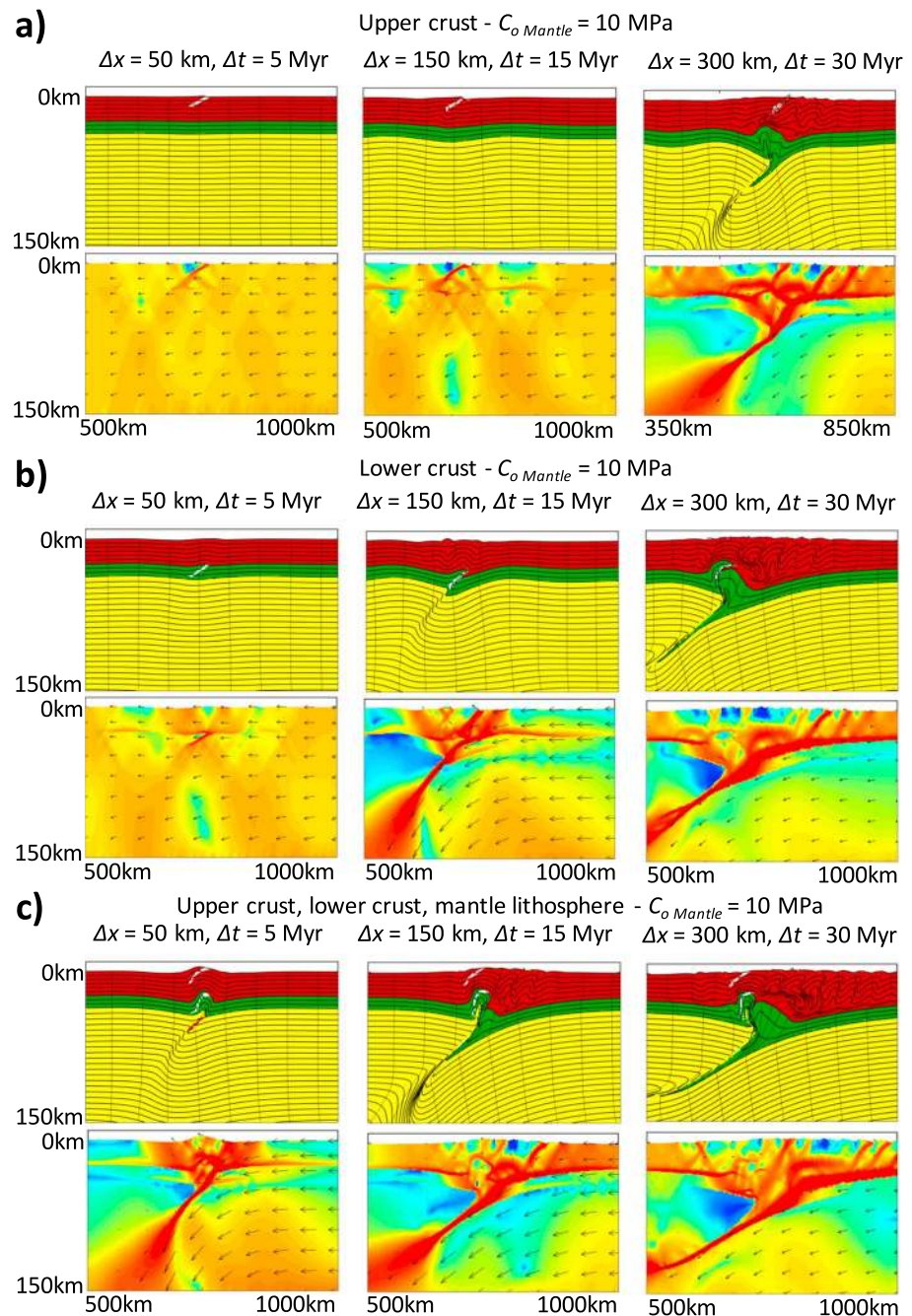
Figure 6. Timings and deformation patterns for scarring in the center of the model with (a) a singular upper crust scar, (b) a singular lower crust scar, and (c) upper crust, lower crust, and mantle lithosphere scar (yellow and red lines, Figure 2b). Material and strain rate plots are given at 5, 15, and 30 Myr.

scar taking only 150 km (Figure 6b). However, a mantle lithosphere scar generates a mantle lithosphere shear almost immediately after shortening commences (Figure 6c).

3.2. Crustal Dominance: Scar Weakness and Moho Temperature

Figures 7 and 8 explore parameters that enable a change in deformation style (from mantle to crust). Previous models have the mantle lithosphere weak scar with an internal angle of friction the same as the crustal heterogeneities ($\phi = 1°$). Figure 7 shows the progression of tectonic deformation when ϕ_{ml} is increased for the mantle lithosphere scars, so that it is not as "weak" as the crustal heterogeneities, alongside changing the strength (f_{ml}) of the mantle lithosphere. For the standard model ($f_{ml} = 1.0$ and $f_{lc} = 0.05$), the mantle litho-
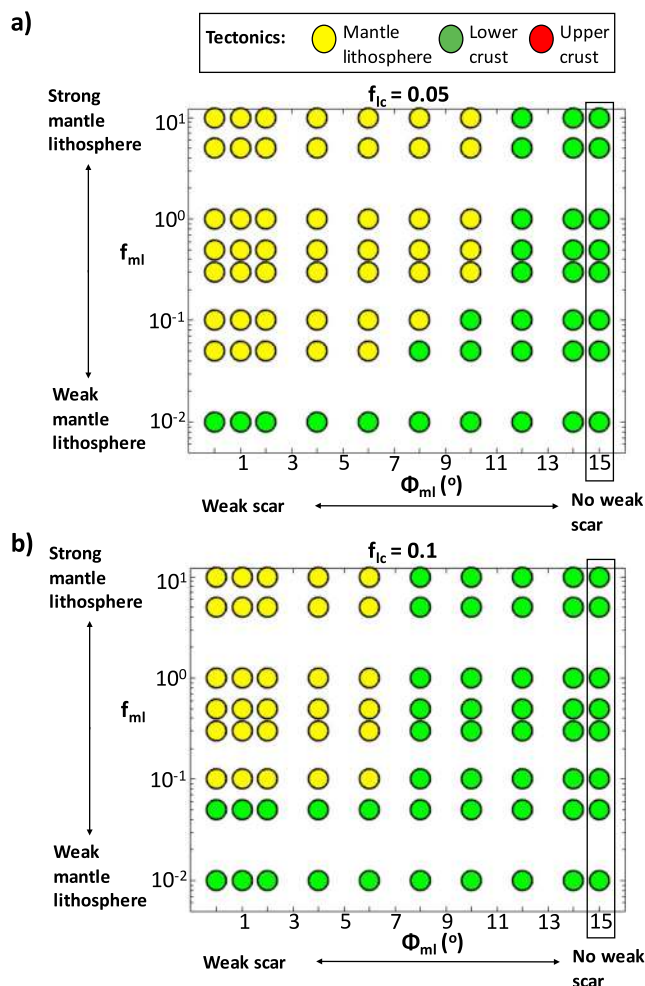
Figure 7. Analyzing the strength of the mantle lithosphere and its weak scar. (a) For $f_{lc} = 0.05$ (the reference case), the weakness of the mantle lithosphere scar (angle of internal friction ϕ_{ml}) as a function of mantle lithosphere strength (as controlled by the scaling function f_{ml}). (b) As above but for an increased lower crust strength ($f_{lc} = 0.1$). When $\phi_{ml} = 15°$, only UC and LC scars are present.

sphere scar dominates tectonics up until $\phi_{ml} = 12°$. Above this value, crustal tectonics related to lower crust scars generate deformation (Figure 7a).

The rheological strength of the mantle lithosphere aids the ability of its scar to control deformation, despite an increased ϕ_{ml}. This result is shown in Figure 7a by mantle lithosphere deformation occurring at lower ϕ_{ml} when f_{ml} is decreased. Accordingly, as the lower crust strength is increased to $f_{lc} = 0.1$ (Figure 7b), crustal deformation occurs at lower ϕ_{ml} and at stronger mantle lithosphere values.

In identifying that the strength of the layers is important (Figures 5 and 7), a suite of models changing the temperature of the crust-mantle boundary (Moho) is presented alongside a changing mantle lithosphere rheology. In Figure 8, shortening models are analyzed for a weak to strong mantle lithosphere and a cold to hot Moho. The ML scars in the models in Figure 8 have the standard $f_{lc} = 0.05$ with $\phi_{ml} = 1°$ (in Figure 8a) and $\phi_{ml} = 12°$ (in Figure 8b).

Figure 8a shows the progression of tectonic styles as the temperature of the Moho is increased. For $f_{ml} = 0.5$, the ML scar dominates tectonics until the Moho temperature reaches 800°C, where the UC scars begin to govern deformation (Figure 8c). However, increasing the f_{ml} to 1.0 at a Moho temperature of 800°C reverts the tectonics to being controlled by the ML scar.

The reason for the deformation can be explained by rheological strength and the brittle-ductile transition based on the temperature-dependent flow. For $f_{ml} = 0.5$, the brittle UC tectonics dominates as the mantle
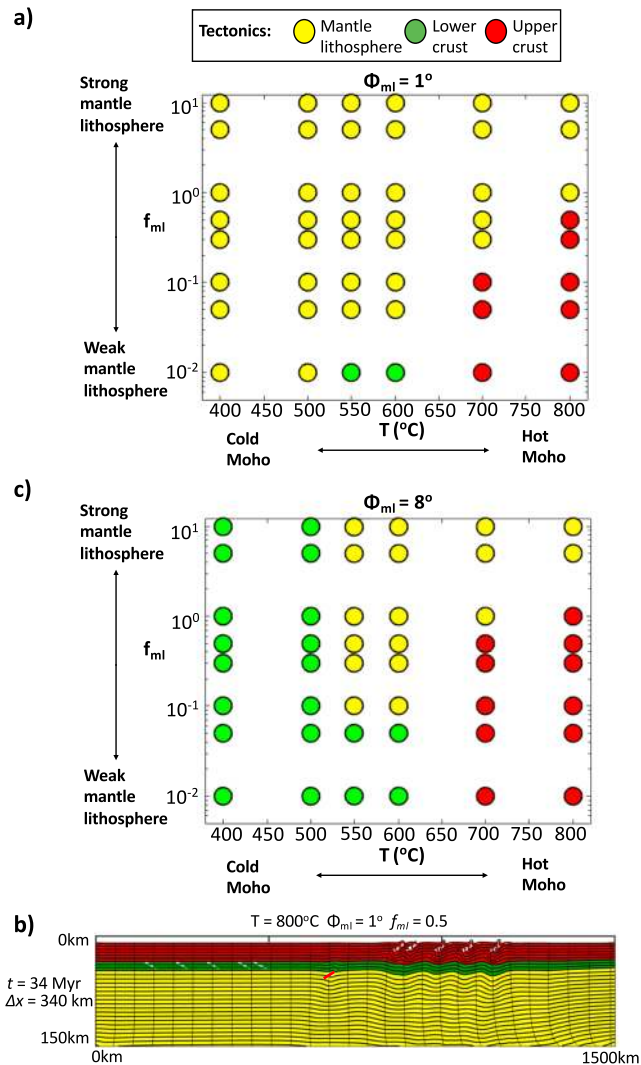
Figure 8. Changing the thermal properties of the model. Moho temperature as a function of mantle lithosphere strength f_{ml} for a model with all UC, LC, and ML scars. The UC and LC scars have $\phi = 1°$, while the ML scars are given as (a) $\phi = 1°$ and (b) $\phi = 8°$. (c) A material field snapshot of $T = 800°C$, $f_{ml} = 0.5$, and $\phi_{ml} = 1°$, showing no transmission of deformation between cold crust and hot mantle after 340 km of shortening.

lithosphere is ductile and weaker. However, for $f_{ml} = 0.1$, the ductile mantle lithosphere where the scar is situated is actually stronger than the brittle UC, and therefore, the heterogeneities within the ML layer control the deformation patterns. This same process occurs in all other models, highlighted by the suite of simulations for $f_{ml} = 0.01$, where the tectonic deformation is controlled by the ML for a cold Moho, then the LC for 550–600°C Moho temperature, and finally UC for a hot Moho (Figure 8a).

Figure 8b shows the change in tectonic style when $\phi_{ml} = 8°$. For the standard mantle lithosphere strength and Moho temperature at this scar weakness ($f_{ml} = 1.0$ and 550° C), the mantle lithosphere dominates tectonics (Figure 7a). However, as the Moho temperature decreases to 500°C and below, the lower crust becomes stronger than the jelly sandwich rheology shown in Figure 3 and controls the deformation pattern (due to the weaker ML scar). As the Moho temperature increases, the strength of the brittle upper crust dominates all (Figure 8b).

Figure 8c shows the different style of intraplate deformation when the Moho temperature is high. Despite the large amount of shortening (340 km), there is no transmission of deformation between "cold" upper crust and hot, ductile mantle. Upper crustal tectonics leading to mantle shearing, as shown in Figure 5a, is not present for hot orogens.
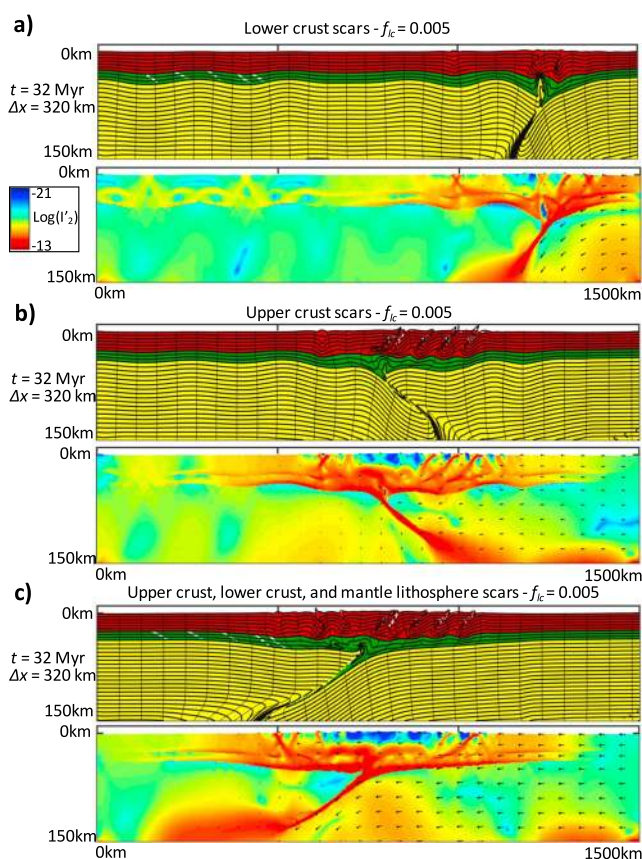
Figure 9. Transmission of deformation to the mantle lithosphere in the presence of a ductile lower crust ($f_{lc} = 0.005$). Deformation relating to (a) lower crust scars only, (b) upper crust scars only, and (c) crustal and mantle lithosphere scars after 320 km of shortening featuring a weakened lower crust.

3.3. Transmitting Through the Jelly: Lower Crust Analysis

The ability of the lower crust jelly to impact the strong mantle lithosphere is explored in Figure 9 where the LC strength is reduced to a purely ductile layer ($f_{lc} = 0.005$). For a shortening model with only lower crust scars (Figure 9a), the deformation pattern reverts back to the reference case (featuring no lithosphere scars) (e.g., Figure 4a). The lower crust scars within the ductile layer have no impact on the tectonic evolution (similar to the findings of Figure 5).

For models featuring only upper crust scars (Figure 9b), we see similar deformation to that of our standard model (with a nonductile LC) in Figure 4b. The deformation of the upper crust transmits through to the mantle lithosphere. Although the lower crust is not as thickened as the standard model (which is in keeping with previous modeling by, e.g., *Rey and Houseman* [2006]), mantle lithosphere shearing does occur after considerable compression.

The presence of a mantle lithosphere scar with shallower crustal heterogeneities (Figure 9c) produces mantle shearing and also subdued lower crustal topography. Orogenesis for models featuring a very weak lower crust is not as localized as the standard models. However, the transmission through the ductile layer to generate similar deformation patterns in Figures 9b and 9c indicates the importance of mantle lithosphere strength in tectonic evolution.

3.4. Deformation Style: Mantle Lithosphere Strength

It is important to note that the different rheological parameters and geometries can generate different deformation patterns. In Figure 10 we present timings and deformation patterns for models that feature a high value of mantle lithosphere cohesion (300 MPa) [e.g., *Gerbault et al.*, 2003] in comparison to the lower $C_o = 10$ MPa in our standard models.
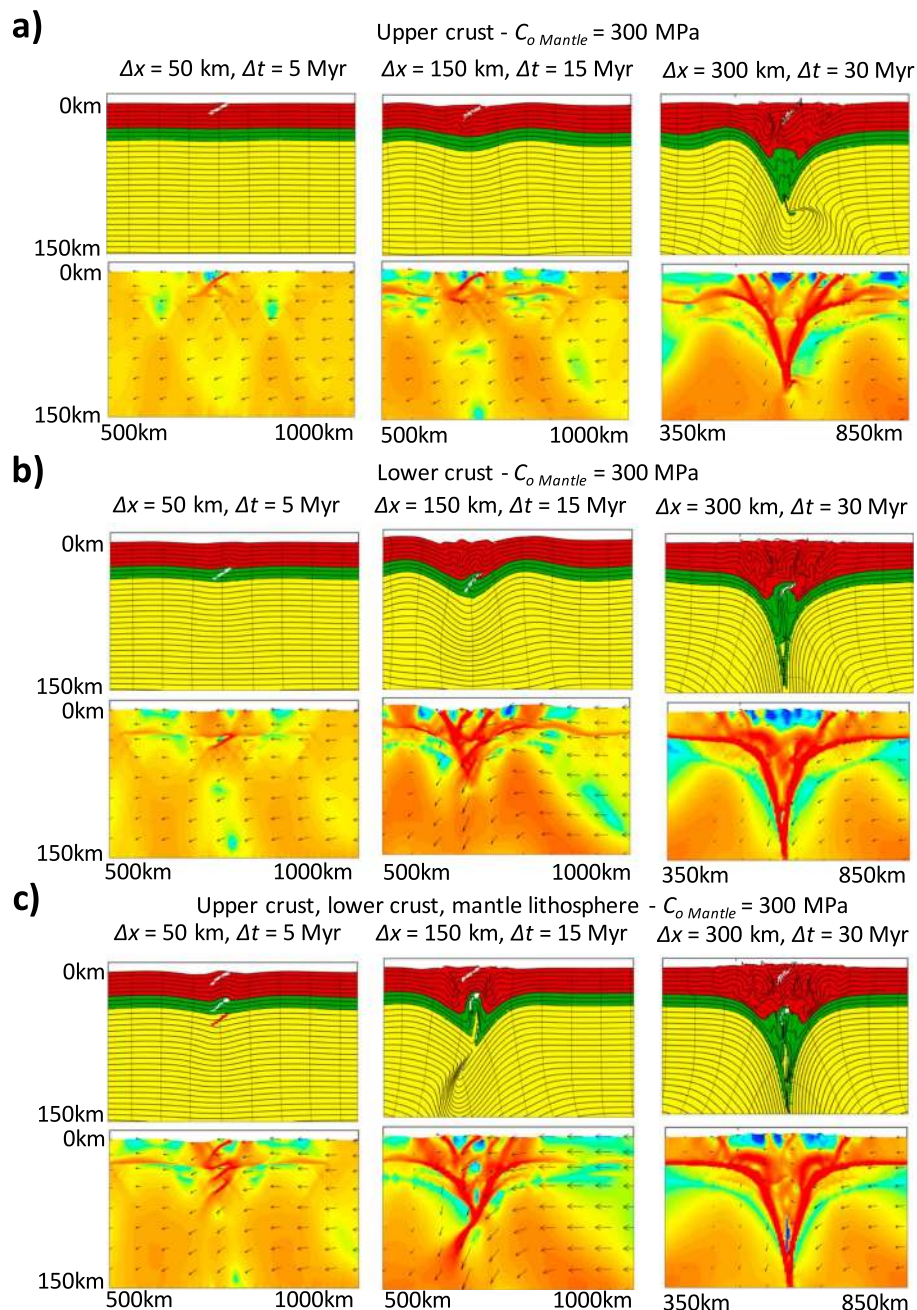
Figure 10. Timings and deformation patterns for scarring in the center of the model that features a high cohesive mantle lithosphere, with (a) a singular upper crust scar, (b) a singular lower crust scar, and (c) upper crust, lower crust, and mantle lithosphere scar (yellow and red lines, Figure 2b). Material and strain rate plots are given at 5, 15, and 30 Myr.

The impact of the high cohesion value of the mantle lithosphere is to produce "dripping" features, dragging the crust vertically. This pattern of deformation could be described as "pop-down" tectonics (Figure 10), as discussed in *Cagnard et al.* [2006a, 2006b], *Chardon et al.* [2009], and *Gapais et al.* [2009, 2014]. The timings of lithosphere scale deformation are similar to that of the standard model (Figure 6).

4. Discussion

Results from our numerical modeling show the importance of lithosphere rheology in intraplate orogenesis and highlight the difficulty in determining the mechanisms for deformation.

We show that a weak scar within the strongest brittle layer can control tectonic evolution, trumping all other heterogeneities (Figure 4d). Weak scars become insignificant within a ductile flow regime and/or within hot mantle regions (Figures 5 and 8). A jelly sandwich rheology is most often used to describe continental lithosphere, and our models indicate that a very weak lower crust can still facilitate deformation in layers above and below (Figure 9). Furthermore, changing the rheology of the mantle lithosphere, when it is the strongest lithospheric layer, is shown to also change the tectonic evolution (Figure 10). A cohesive mantle lithosphere can produce pop-down deformation patterns, previously only discussed in terms of hot orogens in early plate tectonics.

4.1. Intraplate Orogenesis

Our results highlight that while many plate tectonic processes can leave lasting impressions below the crust, these inherited structures within the mantle lithosphere have the potential to influence deformation. This bidirectional pathway of influence from crust to mantle lithosphere can create a geodynamic feedback system (Figure 1). Our models show this system in a number of different ways, with mantle lithosphere scars from ancient tectonics producing crustal deformation (Figure 6c) and crust-driven orogenesis leading to mantle lithosphere shearing (Figures 6a and 6b).

Our models can be interpreted over a broad range of geological settings as our mantle lithosphere-driven deformation pattern generates familiar orogenesis features (e.g., crustal thickening) [e.g., *Murphy et al.*, 1997; *Roberts and Houseman*, 2001; *Collins*, 2002; *Pysklywec and Beaumont*, 2004; *Jammes and Huismans*, 2012; *Wang et al.*, 2013]. To this end, we satisfy a "proof of concept" criteria [e.g., *Jamieson and Beaumont*, 2013] and justify our models to not be purely "geofantasy."

The original question posed was whether previous tectonics can generate inheritance at all lithosphere depths, and if inheritance can control future tectonics, then how can we identify what is driving deformation? Our models suggest that the strongest layer would be the most important and produce deformation with little time to build up strain (e.g., Figure 6c). Although previous studies into orogenesis have inferred that the strongest layer (e.g, mantle lithosphere) would control deformation patterns [e.g., *Bird and Gratz*, 1990; *Buck*, 1991; *Cloetingh et al.*, 2005; *Sokoutis and Willingshofer*, 2011; *Willingshofer et al.*, 2013; *Calignano et al.*, 2015a, 2015b; *Heron et al.*, 2016], our work adds to the discussion with an analysis of the role of a Moho temperature, lower crust strength, and tectonic evolution. The results show that timing and amount of shortening could be important in differentiating between crustal- and mantle-driven lithosphere deformations. Furthermore, a purely ductile lower crust can still transmit deformation between the upper crust and mantle lithosphere, if the mantle lithosphere is strong. A comparison between a jelly sandwich rheology (Figure 9c) and a crème brûlée rheology (Figure 8c) shows this difference in tectonics related to lithosphere strength and highlights the importance of understanding continental rheology.

4.2. Mantle Lithosphere Rheology

Through exploring the range of acceptable parameters for mantle lithosphere rheology within a continent, we found a change in deformation style when increasing C_o (Figure 10). The generation of vertical crustal deformation in these models is similar to pop-down tectonics related to hot orogens with weak lower crust and mantle lithosphere [*Cagnard et al.*, 2006a, 2006b; *Chardon et al.*, 2009; *Gapais et al.*, 2009, 2014]. As a result, the role of the mantle lithosphere in the mechanics of pop-down tectonics may need to be considered in further detail.

By modifying the weakness of the lithospheric scar (through changing ϕ_{ml}), Figure 7 shows that "strong" structural heterogeneities (e.g., a weak zone with a high ϕ_{ml} value) that are within a strong mantle lithosphere are enough to control tectonics over crustal anomalies otherwise primed for failure. In our models, scars within ductile flow would not reactivate.

In the geological record, the reactivation of mantle lithosphere scars is difficult to interpret with certainty. Localized deformation related to deep structural anomalies requires unraveling of tectonic processes. Our results imply that mantle lithosphere scars would not control tectonics in a crème brûlée rheology and/or if the Moho temperature was extremely high (Figure 8). Continental regions that have an appropriate jelly sandwich rheology and Moho temperature, and also feature mantle lithosphere heterogeneities, require a far-field compression to generate deformation. The continental collision of India and Eurasia has generated shortening at the plate boundary but also at a distance away causing intraplate deformation [*Cowgill et al.*, 2003].

Such far-field forcing could be a good reference for determining the horizontal stresses required to reactivate the lithospheric structures that remain in the region from successive continental suturing [e.g., *Watson et al.*, 1987].

World heat flow [e.g., *Davies*, 2013] and stress field maps [e.g., *Heidbach et al.*, 2007] could be used in conjunction with mantle lithosphere scar maps [*Steer et al.*, 1998] to identify potential intraplate regions (of jelly sandwich rheology) where deep structures may control deformation. However, studies into earthquake distribution have proposed that continental mantle lithosphere could behave in a ductile manner, with most of the strength of the lithosphere residing in the upper crust (e.g., a crème brûlée rheology) [*Déverchère et al.*, 2001; *Jackson*, 2002; *Maggi et al.*, 2000]. Nevertheless, the majority of the numerical models presented here are based on stable continents having a jelly sandwich rheology [e.g., *Burov and Watts*, 2006]. Laboratory flow laws indicate that the mantle lithosphere would have a complex layering of brittle and ductile material [e.g., *Brace and Kohlstedt*, 1980; *Sawyer*, 1985; *Gueydan et al.*, 2014], with a broad consensus in the literature indicating that the mantle lithosphere would be strong enough to support high stresses. Therefore, from our models, we would argue that heterogeneities in the mantle lithosphere are important features in plate tectonics and not inconsequential features within a weak layer [e.g., *Déverchère et al.*, 2001; *Jackson*, 2002; *Maggi et al.*, 2000].

Afonso and Ranalli [2004] outlined that neither a jelly sandwich nor seismogenic crust model should be applied to study the continental lithosphere generally and instead that studies would benefit from local analysis. However, for reactivation within relatively stable continents, the arena for this study, *Afonso and Ranalli* [2004] indicate that a jelly sandwich rheology would be applicable. Furthermore, analysis of the 2013 Wind River mantle lithosphere depth earthquake in Wyoming suggests a tectonic event of simple brittle failure at relatively high temperatures [*Craig and Heyburn*, 2015]. The mechanisms for such an earthquakes are unclear, but the region has ancient tectonic activity [*Chamberlain et al.*, 2003] that may have left mantle impressions [e.g., *Hopper and Fischer*, 2015].

Although there are a limited number of deep earthquakes within the mantle lithosphere that have been confirmed [*Zandt and Richins*, 1979; *Sloan and Jackson*, 2012; *Craig and Heyburn*, 2015], improved techniques may be able to better resolve the depth of more events. Furthermore, stable continental lithosphere has also been shown to store elastic strain on long timescales [*Thielmann et al.*, 2015] and when released can generate intermittent intraplate earthquakes [*Craig et al.*, 2016]. Therefore, the mantle lithosphere is a viable candidate for controlling deformation through inherited structure reactivating. A further exploration into the role of elasticity in the mantle lithosphere is required, highlighted by recent thermoelastic-plastic numerical experiments showing strain localization in the lithosphere when compared to thermoplastic models [*Jaquet et al.*, 2016].

4.3. Dimensionality

In our models, the very initiation of shortening generates deformation through mantle lithosphere faulting. However, a considerable amount of stress would be required to produce any shortening on a strong continental interior, while the orientation of scarring with respect to stress field would also be an important factor for reactivation [*Zoback*, 1992; *Heidbach et al.*, 2007]. Our study applies angled scarring in the mantle lithosphere to simulate the reflection features inferred to be relic subduction zones [e.g., *Flack and Warner*, 1990; *Lie and Husebye*, 1994; *Calvert et al.*, 1995; *Cook et al.*, 1999; *White et al.*, 2003; *Schiffer et al.*, 2014, 2015, 2016]. However, other geometries of mantle lithosphere heterogeneities also exist in the geological record [e.g., horizontal reflectors e.g., *Yang*, 2003, and near vertical anomalies e.g., *Gu et al.*, 2015]. Figure 11 shows end-member cases of horizontal, vertical, and cubed scars in the mantle lithosphere for our standard model (e.g., Figure 4).

A vertical ML scar produces similar results to the standard angled models (Figure 11a). However, a cubed weak zone produces pop-down tectonics (Figure 11b), inferring that changing the geometry of mantle lithosphere scars does change the pattern of crustal deformation. The strength contrast of a weaker material next to a strong material is again shown to be important in generating deformation. Figure 11d implements a long (500 km) horizontal ML weak zone that deforms at its extremities. This localization of deformation from a horizontally extensive weak zone would add further complexity in unraveling the epicenter of tectonics in geological examples.

It is important to note that in our models such horizontal weakness in the mantle lithosphere is not reactivated when in the presence of dipping crustal faults (Figure 11e). Lower crust deformation dominates the models
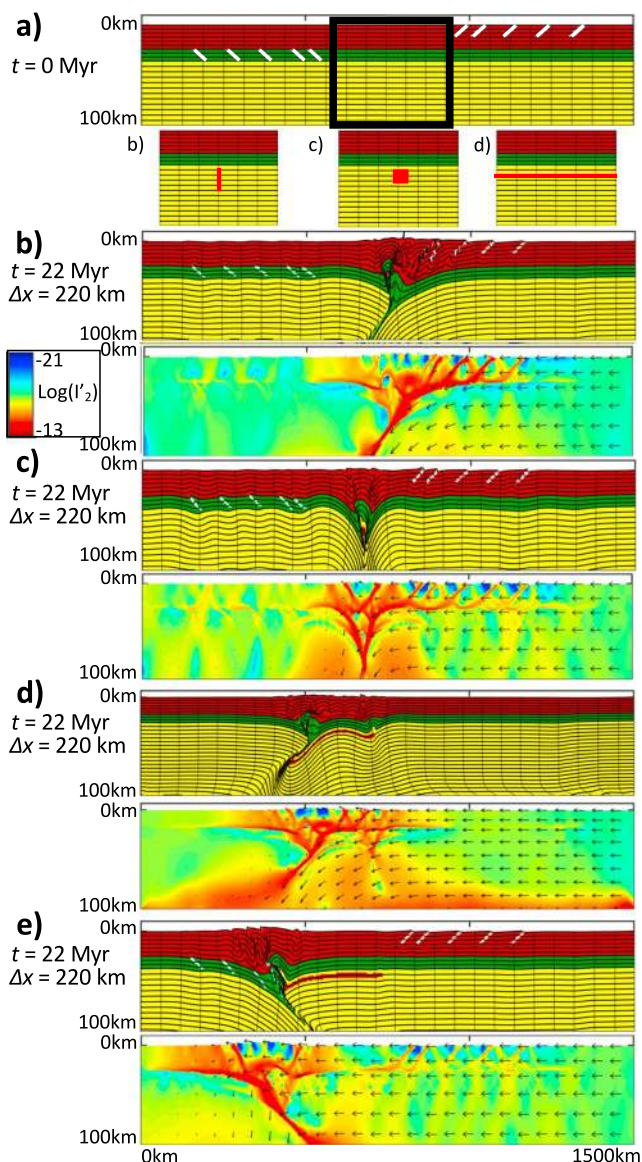
Figure 11. Compression model results for different mantle lithosphere scar geometries using the standard rheological set up (Table 1), with a compression velocity of 1 cm yr^{-1}. (a) The material plot of the upper crust and lower crust scars with black box representing the region where mantle lithosphere scar will be modified (with corresponding geometry shown below). Material deformation (top) and visualization of the second invariant of the deviatoric strain rate tensor (bottom) after extension for models with (b) a vertical and (c) cubed mantle lithosphere scar, (d) a singular horizontal mantle lithosphere scar (no crustal heterogeneities), and (e) a horizontal mantle lithosphere scar featuring crustal heterogeneities. Top 100 km of the models are shown in a 3X vertical exaggeration.

with the horizontal ML scar having a passive role in tectonics. This highlights the importance of continuing to know more about mantle lithosphere structure through deep seismic reflection and receiver function studies.

Understanding the transfer of stress across continental interiors and the optimal orientation of fault reactivation due to horizontal forcing (and horizontal velocity) are beyond the scope of this study. Future work into the role of horizontal velocity and far-field forcing on the reactivation of deep structures would be insightful. Furthermore, an expansion into three dimensions for the numerical experiments would generate more complex structures in the crustal deformation. A recent high-density seismometer array study showed lithospheric variations in the upper mantle to be less than 20 km in width [*Kahraman et al.*, 2015]. As a result, our models implement structures with a 10 km width in the mantle lithosphere. However, the current numerical
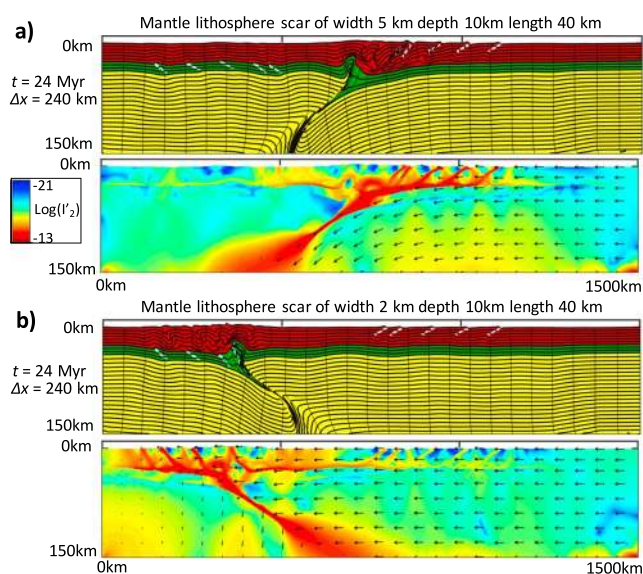
Figure 12. Reduction in resolution of the mantle lithosphere scars for the standard case of crustal and mantle lithosphere weak zones under compression. Material and strain rate plots given for (a) mantle lithosphere scar of half the width of standard case (5 km) and (b) mantle lithosphere scar of a fifth of the width of standard case (2 km). The small resolution of the (Figure 12b) scar makes it ineffectual, and lower crust deformation dominates.

expense to conduct 3-D simulations would not permit the high resolution in the crust and mantle lithosphere structures that is required (and presented here in two dimensions).

Figure 12 shows the resolution limits of the models. The width of the mantle lithosphere scar is halved from 10 km in our standard model to 5 km in Figure 12a and then to 2 km in Figure 12b. Although the mantle lithosphere scar has half the width of the crustal scars in Figure 12a, it still dominates tectonics. However, the lower crust controls deformation in Figure 12b as the mantle scar becomes too small to be resolved.

5. Conclusions

With respect to the Wilson Cycle, we contend that the role of the mantle lithosphere and autogenous inherited structures (Figure 1) is important but has not been sufficiently studied. Our models suggest that lasting impressions on the mantle lithosphere may control intraplate deformation and indeed tectonic processes of the Wilson Cycle driven by inheritance. However, the difficulty in identifying the most prominent layer within the lithosphere is complicated by the failure of coherent tectonic signatures to develop (Figure 1). For instance, crust- and mantle-driven deformations from inherited structures can produce similar patterns of deformation (i.e., mantle lithosphere shearing and crustal thickening) (Figures 4 and 6).

Refining measurements and estimates of continental rheology will help to determine whether the mantle lithosphere has the strongest influence on plate tectonics. The combination of the recent increase in studies showing mantle lithosphere to have long-lived heterogeneities [e.g., *Schiffer et al.*, 2014; *Zhang et al.*, 2014; *Schiffer et al.*, 2015; *Hopper and Fischer*, 2015; *Kahraman et al.*, 2015; *Schiffer et al.*, 2016; *Gilligan et al.*, 2016] and the growing acceptance of the influence of the mantle lithosphere on surface tectonics [*Bercovici and Ricard*, 2014; *Leng and Gurnis*, 2015; *Heron et al.*, 2015b; *Becker et al.*, 2015; *Chamberlain et al.*, 2014; *VanderBeek et al.*, 2016; *Heron and Pysklywec*, 2016; *Heron et al.*, 2016] allows our work to promote a more formal discussion of the mantle lithosphere's place in plate tectonics (and in particular, the Wilson Cycle).

Our study shows that heterogeneities in the mantle lithosphere not only can be generated by crustal tectonics but also influence surface deformation for a wide range of continental rheology. We posit that if the mantle lithosphere is strong with ubiquitous zones of inherited weakness, it is a viable candidate to be the fundamental control on the Wilson Cycle (Figure 1).

References

Afonso, J. C., and G. Ranalli (2004), Crustal and mantle strengths in continental lithosphere: Is the jelly sandwich model obsolete?, *Tectonophysics*, *394*(3–4), 221–232, doi:10.1016/j.tecto.2004.08.006.

Audet, P., and R. Bürgmann (2011), Dominant role of tectonic inheritance in supercontinent cycles, *Nat. Geosci.*, *4*, 184–187, doi:10.1038/ngeo1080.

Avouac, J. P., P. Tapponnier, M. Bai, H. You, and G. Wang (1993), Active thrusting and folding along the northern Tien Shan and Late Cenozoic rotation of the Tarim relative to Dzungaria and Kazakhstan, *J. Geophys. Res.*, *98*(B4), 6755–6804.

Bajolet, F., J. Galeano, F. Funiciello, M. Moroni, A.-M. Negredo, and C. Faccenna (2012), Continental delamination: Insights from laboratory models, *Geochem. Geophys. Geosyst.*, *13*, Q02009, doi:10.1029/2011GC003896.

Beaumont, C., R. A. Jamieson, M. H. Nguyen, and S. Medvedev (2004), Crustal channel flows: 1. Numerical models with applications to the tectonics of the Himalayan-Tibetan orogen, *J. Geophys. Res.*, *109*, B06406, doi:10.1029/2003JB002809.

Becker, T. W., A. R. Lowry, C. Faccenna, B. Schmandt, A. Borsa, and C. Yu (2015), Western U.S. intermountain seismicity caused by changes in upper mantle flow, *Nature*, *524*, 458–461.

Bercovici, D., and Y. Ricard (2014), Plate tectonics, damage and inheritance, *Nature*, *508*, 513–516.

Bird, P. (1979), Continental delamination and the Colorado Plateau, *J. Geophys. Res.*, *84*, 7561–7571.

Bird, P., and A. J. Gratz (1990), A theory for buckling of the mantle lithosphere and Moho during compressive detachments in continents, *Tectonophysics*, *177*, 325–336.

Brace, W. F., and D. L. Kohlstedt (1980), Limits on the lithospheric stress imposed by laboratory experiments, *J. Geophys. Res.*, *85*, 6248–6252.

Buck, W. R. (1991), Modes of continental lithospheric extension, *J. Geophys. Res.*, *96*, 20,161–20,178.

Buiter, S. J. H., A. Y. Babeyko, S. Ellis, T. V. Gerya, B. J. P. Kaus, A. Kellner, G. Schreurs, and Y. Yamada (2006), The numerical sandbox: Comparison of model results for a shortening and an extension experiment, in *Analogue and Numerical Modelling of Crustal-Scale Processes*, vol. 253, edited by S. J. H. Buiter and G. Schreurs, pp. 29–64, Geol. Soc. Spec. Publ., London.

Buiter, S. J. H., O. A. Pfiffner, and C. Beaumont (2009), Inversion of extensional sedimentary basins: A numerical evaluation of the localisation of shortening, *Earth Planet. Sci. Lett.*, *288*, 492–504, doi:10.1016/j.epsl.2009.10.011.

Buiter, S. J. H., et al. (2016), Benchmarking numerical models of brittle thrust wedges, *J. Struct. Geol.*, doi:10.1016/j.jsg.2016.03.003, in press.

Bull, A. L., A. K. McNamara, and J. Ritsema (2009), Synthetic tomography of plume clusters and thermochemical piles, *Earth Planet. Sci. Lett.*, *278*, 152–162.

Burov, E. B. (2011), Rheology and strength of the lithosphere, *Mar. Pet. Geol.*, *28*, 1402–1443, doi:10.1016/j.marpetgeo.2011.05.008.

Burov, E., and A. B. Watts (2006), The long-term strength of the continental lithosphere: "Jelly sandwich" or "crème brûlée"?, *Geol. Soc. Am. Today*, *16*, 4–10, doi:10.1130/1052-5173.

Cagnard, F., N. Durrieu, D. Gapais, J. P. Brun, and C. Ehlers (2006a), Crustal thickening and lateral flow during compression of hot lithospheres, with particular reference to Precambrian times, *Terra Nova*, *18*, 72–78.

Cagnard, F., J. P. Brun, and D. Gapais (2006b), Modes of thickening of analogue weak lithospheres, *Tectonophysics*, *421*, 145–160.

Calignano, E., D. Sokoutis, E. Willingshofer, F. Gueydan, and S. Cloetingh (2015a), Strain localization at the margins of strong lithospheric domains: Insights from analog models, *Tectonics*, *34*, 396–412, doi:10.1002/2014TC003756.

Calignano, E., D. Sokoutis, E. Willingshofer, F. Gueydan, and S. Cloetingh (2015b), Asymmetric vs. symmetric deep lithospheric architecture of intra-plate continental orogens, *Earth Planet. Sci. Lett.*, *424*, 38–50.

Calvert, A. J., E. W. Sawyer, W. J. Davis, and J. N. Ludden (1995), Archean subduction inferred from seismic images of a mantle suture in the Superior Province, *Nature*, *375*, 670–674.

Calvert, A. J., and J. N. Ludden (1999), Archean continental assembly in the southeastern Superior Province in Canada, *Tectonics*, *18*, 412–429.

Chamberlain, K. R., C. D. Frost, and B. R. Frost (2003), Early Archean to Mesoproterozoic evolution of the Wyoming province: Archean origins to modern lithospheric architecture, *Can. J. Earth Sci.*, *40*, 1357–1374.

Chamberlain, C. J., N. Houlié, T. Stern, and H. Bentham (2014), Lithosphere-asthenosphere interactions near the San Andreas Fault, *Earth Planet. Sci. Lett.*, *399*, 14–20, doi:10.1016/j.epsl.2014.04.048.

Chardon, D., D. Gapais, and F. Cagnard (2009), Flow of ultra-hot orogens: A view from the Precambrian, clues for the Phanerozoic, *Tectonophysics*, *477*, 105–118.

Cloetingh, S., P. A. Ziegler, F. Beekman, P. A. M. Andriessen, L. Matenco, G. Bada, D. Garcia-Castellanos, N. Hardebol, P. Dèzes, and D. Sokoutis (2005), Lithospheric memory, state of stress and rheology: Neotectonic controls on Europe's intraplate continental topography, *Quat. Sci. Rev.*, *24*, 241–304, doi:10.1016/j.quascirev.2004.06.015.

Collins, W. J. (2002), Hot orogens, tectonic switching, and creation of continental crust, *Geology*, *30*, 535–538, doi:10.1130/0091-7613(2002).

Cook, F. A. (2002), Fine structure of the continental reflection Moho, *Geol. Soc. Am. Bull.*, *114*, 64–79.

Cook, F. A., and K. Vasudevan (2003), Are there relict crustal fragments beneath the Moho?, *Tectonics*, *22*(3), 1026, doi:10.1029/2001TC001341.

Cook, F. A., A. J. van der Velden, K. W. Hall, and B. J. Roberts (1999), Frozen subduction in Canada's Northwest Territories: Lithoprobe deep seismic reflection profiling of the western Canadian shield, *Tectonics*, *18*, 1–24.

Cook, F. A., R. M. Clowes, D. B. Snyder, A. J. van der Velden, K. W. Hall, P. Erdmer, and C. Evenchick (2004), Precambrian crust and lithosphere beneath the Northern Canadian Cordillera discovered by LITHOPROBE seismic reflection profiling, *Tectonics*, *23*, TC2010, doi:10.1029/2002TC001412.

Cowgill, E., A. Yin, T. M. Harrison, and W. Xiao-Feng (2003), Reconstruction of the Altyn Tagh fault based on U-Pb geochronology: Role of back thrusts, mantle sutures, and heterogeneous crustal strength in forming the Tibetan Plateau, *J. Geophys. Res*, *108*, 2346, doi:10.1029/2002jb002080.

Craig, T. J., and R. Heyburn (2015), An enigmatic earthquake in the continental mantle lithosphere of stable North America, *Earth Planet. Sci. Lett.*, *425*(2015), 12–23.

Craig, T. J., E. Calais, L. Fleitout, L. Bollinger, and O. Scotti (2016), Evidence for the release of long-term tectonic strain stored in continental interiors through intraplate earthquakes, *Geophys. Res. Lett.*, *43*, 6826–6836, doi:10.1002/2016GL069359.

Davies, J. H. (2013), Global map of solid Earth surface heat flow, *Geochem. Geophys. Geosyst.*, *14*, 4608–4622, doi:10.1002/ggge.20271.

Davis, M., and N. Kusznir (2004), Depth-dependent lithospheric stretching at rifted continental margins, *Proc. NSF Rifted Margins Theor. Inst.*, *1*, 92–136.

Déverchère, J., C. Petit, N. Gileva, N. Radziminovitch, V. Melnikova, and V. Sankov (2001), Depth distribution of earthquakes in the Baikal rift system and its implications for the rheology of the lithosphere, *Geophys. J. Int.*, *146*, 714–730.

Dewey, J. F., and K. Burke (1974), Hot spots and continental breakup: Implications for collisional orogeny, *Geology*, *2*, 57–60, doi:10.1130/0091-7613.

Dèzes, P., S. M. Schmid, and P. A. Ziegler (2004), Evolution of the European Cenozoic Rift System: Interaction of the Alpine and Pyrenean orogens with their foreland lithosphere, *Tectonophysics*, *389*, 1–33, doi:10.1016/j.tecto.2004.06.011.

Dunbar, J. A., and D. S. Sawyer (1988), Continental rifting at pre-existing lithospheric weaknesses, *Nature*, *333*, 450–452.

Dunbar, J. A., and D. S. Sawyer (1989), How preexisting weaknesses control the style of continental breakup, *J. Geophys. Res.*, *94*, 7278–7292.

Ernst, R. E., K. L. Buchan, and I. H. Campbell (2005), Frontiers in large igneous province research, *Lithos*, *79*, 271–297.

Flack, C., and M. Warner (1990), Three-dimensional mapping of seismic reflections from the crust and upper mantle, northwest of Scotland, *Tectonophysics*, *173*, 469–481.

Fullsack, P. (1995), An arbitrary Lagrangian-Eulerian formulation for creeping flows and its application in tectonic models, *Geophys. J. Int.*, *120*(1), 1–23, doi:10.1111/j.1365-246X.1995.tb05908.x.

Gapais, D., F. Cagnard, F. Gueydan, P. Barbey, and M. Ballèvre (2009), Mountain building and exhumation processes through time: Inferences from nature and models, *Terra Nova*, *21*, 188–194.

Gapais, D., J. Jaguin, F. Cagnard, and P. Boulvais (2014), Pop-down tectonics, fluid channelling and ore deposits within ancient hot orogens, *Tectonophysics*, *618*, 102–106.

Gerbault, M., S. Henrys, and F. Davey (2003), Numerical models of lithospheric deformation forming the Southern Alps of New Zealand, *J. Geophys. Res.*, *108*(B7), 2341, doi:10.1029/2001JB001716.

Ghazian, R. K., and S. J. H. Buiter (2013), A numerical investigation of continental collision styles, *Geophys. J. Int.*, *193*, 1133–1152.

Gilligan, A., I. D. Bastow, and F. A. Darbyshire (2016), Seismological structure of the 1.8 Ga Trans-Hudson Orogen of North America, *Geochem. Geophys. Geosyst.*, *17*, 2421–2433, doi:10.1002/2016GC006419.

Gleason, G. C., and J. Tullis (1995), A flow law for dislocation creep of quartz aggregates determined with the molten salt cell, *Tectonophysics*, *247*, 1–23.

Göğüş, O. H., and R. N. Pysklywec (2008), Mantle lithosphere delamination driving plateau uplift and synconvergent extension in eastern Anatolia, *Geology*, *36*, 723–726, doi:10.1130/G24982A.1.

Göğüş, O. H., R. N. Pysklywec, and C. Faccenna (2016), Postcollisional lithospheric evolution of the Southeast Carpathians: Comparison of geodynamical models and observations, *Tectonics*, *35*, 1205–1224, doi:10.1002/2015TC004096.

Gray, R., and R. N. Pysklywec (2012), Geodynamic models of mature continental collision: Evolution of an orogen from lithospheric subduction to continental retreat/delamination, *J. Geophys. Res.*, *117*, B03408, doi:10.1029/2011JB008692.

Gu, Y. J., Y. Zhang, M. D. Sacchi, Y. Chen, and S. Contenti (2015), Sharp mantle transition from cratons to Cordillera in southwestern Canada, *J. Geophys. Res. Solid Earth*, 5051–5069, doi:10.1002/2014JB011802.

Guellec, S., D. Lajat, A. Mascle, F. Roure, and M. Tardy (1990), Deep seismic profiling and petroleum potential in the Western Alps: Constraints with ECORS data, balanced cross sections and hydrocarbon modelling, in *The Potential of Deep Seismic Profiling for Hydrocarbon Exploration*, edited by B. Pinet and C. Bois, pp. 425–437, Edition Technip, Paris.

Gueydan, F., J. Précigout, and L. G. J. Montési (2014), Strain weakening enables continental plate tectonics, *Tectonophysics*, *631*, 189–196, doi:10.1016/j.tecto.2014.02.005.

Hansen, D. L., and S. B. Nielsen (2002), Does thermal weakening explain basin inversion?, *Earth Planet. Sci. Lett.*, *198*, 113–127.

Heidbach, O., J. Reinecker, M. Tingay, B. Moeller, B. Sperner, K. Fuchs, and F. Wenzel (2007), Plate boundary forces are not enough: Second- and third-order stress patterns highlighted in the World Stress Map database, *Tectonics*, *26*, TC6014, doi:10.1029/2007TC002133.

Heron, P. J., J. P. Lowman, and C. Stein (2015a), Influences on the positioning of mantle plumes following supercontinent formation, *J. Geophys. Res. Solid Earth*, *120*, 3628–3648, doi:10.1002/2014JB011727.

Heron, P. J., R. N. Pysklywec, and R. Stephenson (2015b), Intraplate orogenesis within accreted and scarred lithosphere: Example of the Eurekan Orogeny, Ellesmere Island, *Tectonophysics*, *664*, 202–213, doi:10.1016/j.tecto.2015.09.011.

Heron, P. J., R. N. Pysklywec, and R. Stephenson (2016), Lasting mantle scars lead to perennial plate tectonics, *Nat. Commun.*, *7*, 11834, doi:10.1038/ncomms11834.

Heron, P. J., and R. N. Pysklywec (2016), Inherited structure and coupled crust-mantle lithosphere evolution: Numerical models of Central Australia, *Geophys. Res. Lett.*, *43*, 4962–4970, doi:10.1002/2016GL068562.

Hess, H. H. (1962), History of ocean basins, in *Petrologic Studies: A Volume in Honor of A. F. Buddington*, edited by A. E. J. Engel, H. L. James, and B. F. Leonard, pp. 599–620, Geol. Soc. Am., New York.

Hirth, G., and D. L. Kohlstedt (1996), Water in the oceanic upper mantle: Implications for rheology, melt extraction and the evolution of the lithosphere, *Earth Planet. Sci. Lett.*, *144*, 93–108.

Hopper, E., and K. M. Fischer (2015), The meaning of midlithospheric discontinuities: A case study in the northern U.S. craton, *Geochem. Geophys. Geosyst.*, *16*, 4057–4083, doi:10.1002/2015GC006030.

Houseman, G. A., and P. Molnar (1997), Gravitational (Rayleigh-Taylor) instability of a layer with non-linear viscosity and convective thinning of continental lithosphere, *Geophys. J. Int.*, *128*, 125–150.

Houseman, G. A., D. P. McKenzie, and P. Molnar (1981), Convective instability of a thickened boundary layer and its relevance for the thermal evolution of continental convergent belts, *J. Geophys. Res.*, 6115–6132.

Huismans, R., and C. Beaumont (2011), Depth-dependent extension, two-stage breakup and cratonic underplating at rifted margins, *Nature*, *473*, 74–78, doi:10.1038/nature09988.

Jackson, J. (2002), Strength of the continental lithosphere: Time to abandon the jelly sandwich?, *Geol. Soc. Am. Today*, *12*(9), 4–10.

Jaquet, Y., T. Duretz, and S. M. Schmalholz (2016), Dramatic effect of elasticity on thermal softening and strain localization during lithospheric shortening, *Geophys. J. Int.*, *204*, 780–784.

Jamieson, R. A., and C. Beaumont (2013), On the origin of orogens, *Geol. Soc. Am. Bull.*, *125*, 1671–1702, doi:10.1130/B30855.1.

Jammes, S., and R. S. Huismans (2012), Structural styles of mountain building: Controls of lithospheric rheologic stratification and extensional inheritance, *J. Geophys. Res.*, *117*, B10403, doi:10.1029/2012JB009376.

Kawazoe, T., S.-I. Karato, K. Otsuka, Z. Jing, and M. Mookherjee (2009), Shear deformation of dry polycrystalline olivine under deep upper mantle conditions using a Rotational Drickamer Apparatus (RDA), *Earth Planet. Sci. Lett.*, *174*, 128–137.

Kahraman, M., D. G. Cornwell, D. A. Thompson, S. Rost, G. A. Houseman, N. Tïkelli, U. Teoman, S. A. Poyraz, M. Utkucu, and L. Gülen (2015), Crustal-scale shear zones and heterogeneous structure beneath the North Anatolian Fault Zone, Turkey, revealed by a high-density seismometer array, *Earth Planet. Sci. Lett.*, *430*, 129–139, doi:10.1016/j.epsl.2015.08.014.

Kelemen, P. B., and G. Hirth (2007), A periodic shear-heating mechanism for intermediate-depth earthquakes in the mantle, *Nature*, *446*(7137), 787–790, doi:10.1038/nature05717.

Klemperer, S., and R. Hobbs (1991), *The BIRPS Atlas, Deep Seismic Reflection Profiles Around the British Isles*, 124 pp., Cambridge Univ. Press, Cambridge, U. K.

Krajcinovic, D. (1996), *Damage Mechanics*, Elsevier Sci., New York.

Lee, C-T, Q-Z Yin, RL Rudnick, and SB Jacobsen (2001), Preservation of ancient and fertile lithospheric mantle beneath the southwestern United States, *Nature*, *411*, 69–73.

Lee, C.-T. A., P. Luffi, and E. Chin (2011), Building and destroying continental mantle, *Annu. Rev. Earth Planet. Sci.*, *39*, 59–90.

Leng, W., and M. Gurnis (2015), Subduction initiation at relic arcs, *Geophys. Res. Lett.*, *42*, 7014–7021, doi:10.1002/2015GL064985.

Lie, J. E., and E. S. Husebye (1994), Simple-shear deformation of the Skagerrak lithosphere during the formation of the Oslo Rift, *Tectonophysics*, *232*, 133–141.

Linckens, J., M. Herwegh, and O. Müntener (2015), Small quantity but large effect? How minor phases control strain localization in upper mantle shear zones, *Tectonophysics*, *643*, 26–43, doi:10.1016/j.tecto.2014.12.008.

Loken, C., et al. (2010), SciNet: Lessons learned from building a power-efficient Top-20 system and data centre, *J. Phys.*, *256*, 12026, doi:10.1088/1742-6596/256/1/012026.

Mackwell, S. J., M. E. Zimmerman, and D. L. Kohlstedt (1998), High-temperature deformation of dry diabase with application to tectonics on Venus, *J. Geophys. Res.*, *103*, 975–984.

Maggi, A., J. A. Jackson, K. Priestley, and C. Baker (2000), A reassessment of focal depth distributions in southern Iran, the Tien Shan and northern India: Do earthquakes really occur in the continental mantle?, *Geophys. J. Int.*, *143*, 629–661.

Mallard, C., N. Coltice, M. Seton, R. D. Muller, and P. J. Tackley (2016), Subduction controls the distribution and fragmentation of Earth's tectonic plates, *Nature*, *535*, 140–143, doi:10.1038/nature17992.

McNamara, A. K., and S. J. Zhong (2005), Thermochemical structures beneath Africa and the Pacific Ocean, *Nature*, *437*, 1136–1139, doi:10.1038/nature04066.

Morgan, J. V., M. Hadwin, M. R. Warner, P. J. Barton, and R. P. L. Morgan (1994), The polarity of deep seismic reflections from the lithospheric mantle: Evidence for a relict subduction zone, *Tectonophysics*, *232*, 319–328.

Mouthereau, F., O. Lacombe, and B. Meyer (2006), The Zagros folded belt (Fars, Iran): Constraints from topography and critical wedge modeling, *Geophys. J. Int.*, *165*, 336–356.

Murphy, M. A., A. Yin, T. M. Harrison, S. B. Durr, Z. Chen, F. J. Ryerson, W. S. F. Kidd, X. Wang, and X. Zhou (1997), Did the Indo-Asian collision alone create the Tibetan Plateau?, *Geology*, *25*, 719–722.

Nance, R. D., and J. B. Murphy (2013), Origins of the supercontinent cycle, *Geosci. Front.*, *4*, 439–448, doi:10.1016/j.gsf.2012.12.007.

Nielsen, S. B., and D. L. Hansen (2000), Physical explanation of the formation and evolution of inversion zones and marginal troughs, *Geology*, *28*, 875–878.

Ogawa, M. (1987), Shear instability in a viscoelastic material as the cause of deep focus earthquakes, *J. Geophys. Res.*, *92*(B13), 13,801–13,810, doi:10.1029/JB092iB13p13801.

Percival, J. A., and R. N. Pysklywec (2007), Are Archean lithospheric keels inverted?, *Earth Planet. Sci. Lett.*, *254*, 393–403.

Péron-Pinvidic, G., G. Manatschal, and P. T. Osmundsen (2013), Structural comparison of archetypal Atlantic rifted margins: A review of observations and concepts, *Mar. Pet. Geol.*, *43*, 21–47.

Pfiffner, O. A. (1992), Alpine orogeny, in *A Continent Revealed: The European Geotraverse*, edited by D. Blundell, R. Freeman, and St. Mliller, pp. 180–190, Cambridge Univ. Press, Cambridge, U. K.

Pollack, H. N. (1986), Cratonization and thermal evolution of the mantle, *Earth Planet. Sci. Lett.*, *80*, 175–182.

Prieto, G. A., M. Florez, S. A. Barrett, G. C. Beroza, P. Pedraza, J. F. Blanco, and E. Poveda (2013), Seismic evidence for thermal runaway during intermediate-depth earthquake rupture, *Geophys. Res. Lett.*, *40*, 6064–6068, doi:10.1002/2013GL058109.

Pysklywec, R. N., and C. Beaumont (2004), Intraplate tectonics: Feedback between radioactive thermal weakening and crustal deformation driven by mantle lithosphere instabilities, *Earth Planet. Sci. Lett.*, *221*, 275–292.

Ranalli, G. (1997), Rheology of the lithosphere in space and time, in *Orogeny Through Time*, vol. 121, edited by J.-P. Burg and M. Ford, pp. 19–37, Geol. Soc. Spec. Publ., London.

Rey, P. F., and G. Houseman (2006), Lithospheric scale gravitational flow: The impact of body forces on orogenic processes from Archaean to Phanerozoic, in *Analogue and Numerical Modelling of Crustal-Scale Processes*, edited by S. J. H. Buiter and G. Schreurs, *Geol. Soc. London, Spec. Publ., 253*, pp. 153–167.

Roberts, E. A., and G. A. Houseman (2001), Geodynamics of central Australia during the intraplate Alice Springs Orogeny: Thin viscous sheet models, *Geol. Soc. London Spec. Publ*, *184*(1), 139–164.

Royden, L., and C. E. Keen (1980), Rifting process and thermal evolution of the continental margin of eastern Canada determined from subsidence curves, *Earth Planet. Sci. Lett.*, *51*, 343–361.

Sandiford, M. (1999), Mechanics of basin inversion, *Tectonophysics*, *305*, 109–120.

Sandiford, M., D. L. Hansen, and S. N. McLaren (2006), Lower crustal rheological expression in inverted basins, in *Analogue and Numerical Modelling of Crustal Scale Processes*, edited by S. Buiter and G. Schreurs, *Geol. Soc. London, Spec. Publ., 253*, pp. 271–283.

Sawyer, D. S. (1985), Brittle failure in the upper mantle during extension of continental lithosphere, *J. Geophys. Res*, *90*, 3021–3025.

Schaeffer, A., and S. Lebedev (2015), Global heterogeneity of the lithosphere and underlying mantle: A seismological appraisal based on multimode surface-wave dispersion analysis, shear-velocity tomography, and tectonic regionalization, in *The Earth's Heterogeneous Mantle*, pp. 3–46, Springer, Switzerland.

Schiffer, C., N. Balling, B. H. Jacobsen, R. A Stephenson, and S. B. Nielsen (2014), Seismological evidence for a fossil subduction zone in the East Greenland Caledonides, *Geology*, *42*, 311–314, doi:10.1130/G35244.1.

Schiffer, C., R. A. Stephenson, K. D. Petersen, S. B. Nielsen, B. H. Jacobsen, and N. Balling (2015), A sub-crustal piercing point for North Atlantic reconstructions and tectonic implications, *Geology*, *43*, 1087–1090, doi:10.1130/G37245.1.

Schiffer, C., N. Balling, J. Ebbing, B. H. Jacobsen, and S. B. Nielsen (2016), Geophysical-petrological modelling of the East Greenland Caledonides—Isostatic support from crust and upper mantle, *Tectonophysics*, doi:10.1016/j.tecto.2016.06.023, in press.

Sibson, R. H. (1992), Implications of fault-valve behaviour for rupture nucleation and recurrence, *Tectonophysics*, *211*, 283–293.

Skemer, P., J. M. Warren, P. B. Kelemen, and G. Hirth (2010), Microstructural and rheological evolution of a mantle shear zone, *J. Petrol.*, *51*, 43–53.

Sloan, R. A., and J. Jackson (2012), Upper-mantle earthquakes beneath the Arafura Sea and south Aru Trough: Implications for continental rheology, *J. Geophys. Res*, *117*, doi:10.1029/2011JB008992.

Smith, R. B., and R. L. Bruhn (1984), Intraplate extensional tectonics of the eastern Basin-Range: Inferences on structural style from seismic reflection data, regional tectonics, and thermal-mechanical models of brittle-ductile deformation, *J. Geophys. Res.*, *89*, 5733–5762, doi:10.1029/JB089iB07p05733.

Sokoutis, D., and E. Willingshofer (2011), Decoupling during continental collision and intra-plate deformation, *Earth Planet. Sci. Lett.*, *305*, 435–444, doi:10.1016/j.epsl.2011.03.028.

Steer, D. N., J. H. Knapp, and D. L. Brown (1998), Super-deep reflection profiling: Exploring the continental mantle lid, *Tectonophysics*, *286*, 111–121.

Stein, S., and M. Liu (2009), Long aftershock sequences within continents and implications for earthquake hazard assessment, *Nature*, *462*, 97–99.

Stephenson, R., D. L. Egholm, S. B. Nielsen, and S. M. Stovba (2009), Role of thermal refraction in localizing intraplate deformation in southeastern Ukraine, *Nat. Geosci.*, *2*, 290–293.

Sykes, L. R. (1972), Seismicity as a guide to global tectonics and earthquake prediction, *Tectonophysics*, *13*, 393–414.

Sykes, L. R. (1978), Intraplate seismicity, reactivation of pre-existing zones of weakness, alkaline magmatism, and other tectonism postdating continental fragmentation, *Rev. Geophys.*, *16*(4), 621–688.

Tapponnier, P., and P. Molnar (1975), Cenozoic tectonics of Asia: Effects of a continental collision, *Science*, *189*(4201), 419–426.

Thielmann, M., B. Kaus, and A. Popov (2015), Lithospheric stresses in Rayleigh-Bernard convection: Effects of a free surface and a visco-elastic Maxwell rheology, *Geophys. J. Int.*, *203*(3), 2200–2219, doi:10.1093/gji/ggv436.

Thomas, W. A. (2006), Tectonic inheritance at a continental margin, *Geol. Soc. Am. Today*, *16*(2), 4–11.

Wang, Y., L. Zhou, and L. Zhao (2013), Cratonic reactivation and orogeny: An example from the northern margin of the North China Craton, *Gondwana Res.*, *24*, 1203–1222.

Wang, H., J. van Hunen, D. G. Pearson, and M. B. Allen (2014), Craton stability and longevity: The roles of composition-dependent rheology and buoyancy, *Earth Planet. Sci. Lett.*, *391*, 224–233.

Warren, J. M., and G. Hirth (2006), Grain size sensitive deformation mechanisms in naturally deformed peridotites, *Earth Planet. Sci. Lett.*, *248*, 438–450.

Watson, M. P., D. N. Hayward, D. N. Parkinson, and Zh. M. Zhang (1987), Plate tectonic history, basin development and petroleum source rock deposition onshore China, *Mar. Petrol. Geol.*, *4*, 205–225.

Wiens, D. A. (2001), Seismological constraints on the mechanism of deep earthquakes: Temperature dependence of deep earthquake source properties, *Phys. Earth Planet. Inter.*, *127*(1), 145–163, doi:10.1016/S0031-9201(01)00225-4.

Wendlandt, E., D. J. DePaolo, and W. S. Baldridge (1993), Nd and Sr isotope chronostratigraphy of Colorado Plateau lithosphere: Implications for magmatic and tectonic underplating of the continental crust, *Earth Planet. Sci. Lett.*, *116*, 23–43.

Willingshofer, E., D. Sokoutis, S. W. Luth, S. W. Beekman, and S. Cloetingh (2013), Subduction and deformation of the continental lithosphere in response to plate and crust-mantle coupling, *Geology*, *41*(12), 1239–1242.

Wilson, J. T. (1965), A new class of faults and their bearing on continental drift, *Nature*, *207*, 343–47.

Wilson, J. T. (1966), Did the Atlantic close and then re-open?, *Nature*, *211*(5050), 676–681.

White, D. J., G. Musacchio, H. H. Helmstaedt, R. M. Harrap, P. C. Thurston, A. van der Velden, and K. Hall (2003), Images of a lower-crustal oceanic slab: Direct evidence for tectonic accretion in the Archean western Superior Province, *Geology*, *31*, 997–1000.

VanderBeek, B., D. R. Toomey, E. E. E. Hooft, and W. S. D. Wilcock (2016), Segmentation of mid-ocean ridges caused by oblique mantle divergence, *Nature Geosci.*, *9*, doi:10.1038/NGEO2745, in press.

van Keken, P. E., S. D. King, H. Schmeling, E. R. Christensen, D. Neumeister, and M.-P. Doin (1997), A comparison of methods for the modeling of thermochemical convection, *J. Geophys. Res.*, *102*, 22,477–22,495.

van der Velden, A. J., and F. A. Cook (2002), Products of 2.65–2.58 Ga orogenesis in the Slave Province correlated with Slave-Northern Cordillera Lithospheric Evolution (SNORCLE) seismic reflection patterns, *Can. J. Earth Sci.*, *38*, 1189–1200.

Vine, F. J., and D. H. Matthews (1963), Magnetic anomalies over oceanic ridges, *Nature*, *199*, 947–49.

van der Velden, A. J., and F. A. Cook (2005), Relict subduction zones in Canada, *J. Geophys. Res.*, *110*, B08403, doi:10.1029/2004JB003333.

Vauchez, A., G. Barruol, and A. Tommasi (1997), Why do continents break up parallel to ancient orogenic belts?, *Terra Nova*, *9*, 62–66.

Vauchez, A., A. Tommasi, and G. Barrruol (1998), Rheological heterogeneity, mechanical anisotropy and deformation of the continental lithosphere, *Tectonophysics*, *296*, 61–86.

Yang, W. C. (2003), Flat mantle reflectors in eastern China: Possible evidence of lithospheric thinning, *Tectonophysics*, *369*, 219–230.

Yuan, H., and B. Romanowicz (2010), Lithospheric layering in the North American craton, *Nature*, *466*, 1063–1068.

Zandt, G., and W. D. Richins (1979), An upper mantle earthquake beneath the middle Rocky Mountains in NE Utah, *Earthquake Notes*, *50*, 69–70.

Zhang, S., et al. (2014), Crustal structures revealed from a deep seismic reflection profile across the Solonker suture zone of the Central Asian Orogenic Belt, northern China: An integrated interpretation, *Tectonophysics*, *612-613*, 26–39.

Ziegler, P. A. (1987), Late Cretaceous and Cenozoic intra-plate compressional deformations in the Alpine foreland—A geodynamic model, *Tectonophysics*, *137*, 389–420.

Ziegler, P. A., S. Cloetingh, and J.-D. van Wees (1995), Dynamics of intra-plate compressional deformation: The Alpine foreland and other examples, *Tectonophysics*, *252*, 7–59.

Ziegler, P. A., J.-D. van Wees, and S. Cloetingh (1998), Mechanical controls on collision-related compressional intraplate deformation, *Tectonophysics*, *300*, 103–129, doi:10.1016/S0040-1951(98)00236-4.

Zoback, M. L. (1992), Stress field constraints on intraplate seismicity in eastern North America, *J. Geophys. Res.*, *97*(B8), 11,761–11,782, doi:10.1029/92JB00221.